

Title Page

Supplement: Bimodal Inference in Humans and Mice

Authors:

Veith Weilnhammer^{1,2}, Heiner Stuke^{1,2}, Kai Standvoss^{1,3,5}, Philipp Sterzer⁶

Affiliations:

¹ Department of Psychiatry, Charité-Universitätsmedizin Berlin, corporate member of Freie Universität Berlin and Humboldt-Universität zu Berlin, 10117 Berlin, Germany

² Berlin Institute of Health, Charité-Universitätsmedizin Berlin and Max Delbrück Center, 10178 Berlin, Germany

³ Bernstein Center for Computational Neuroscience, Charité-Universitätsmedizin Berlin, 10117 Berlin, Germany

⁴ Berlin School of Mind and Brain, Humboldt-Universität zu Berlin, 10099 Berlin, Germany

⁵ Einstein Center for Neurosciences Berlin, 10117 Berlin, Germany

⁶ Department of Psychiatry (UPK), University of Basel, Switzerland

Corresponding Author:

Veith Weilnhammer, Department of Psychiatry, Charité Campus Mitte, Charitéplatz 1, 10117 Berlin, phone: 0049 (0)30 450 517 317, email: veith.weilnhammer@gmail.com

¹ 1 Supplemental Items

² 1.1 Internal mode processing is driven by choice history as opposed ³ to stimulus history

⁴ The main manuscript reports the effects of perceptual history, which we defined
⁵ as the impact of the choice at the preceding trial on the choice at the current trial
⁶ (henceforth *choice history*). *Stimulus history*, which is defined as the impact of
⁷ the stimulus presented at the preceding trial on the choice at the present trial,
⁸ represents an alternative approach to this. Here, we compare the effects of choice
⁹ history to the effects of stimulus history.

¹⁰ We observed a significant bias toward stimulus history (humans: $49.76\% \pm 0.1\%$
¹¹ of trials, $\beta = 1.26 \pm 0.94$, $T(373.62) = 1.34$, $p = 0.18$; mice: $51.11\% \pm 0.08\%$ of
¹² trials, $T(164) = 13.4$, $p = 3.86 \times 10^{-28}$). The bias toward stimulus history was
¹³ smaller than the bias toward choice history (humans: $\beta = -3.53 \pm 0.5$, $T(66.53)$
¹⁴ $= -7.01$, $p = 1.48 \times 10^{-9}$; mice: $T(164) = -17.21$, $p = 1.43 \times 10^{-38}$).

¹⁵ The attraction of choices toward both preceding choices and stimuli is expected,
¹⁶ as perception was *stimulus-congruent* on approximately 75% of trials, causing
¹⁷ choices and stimuli to be highly correlated. We therefore compared the effects
¹⁸ of choice history and stimulus history after *stimulus-incongruent* (i.e., *error*)
¹⁹ trials, since those trials lead to opposite predictions regarding the perceptual
²⁰ choice at the subsequent trial.

²¹ As expected from the findings presented in the main manuscript, perceptual
²² choices were attracted toward perceptual choices when the inducing trial was
²³ stimulus-incongruent (i.e., a positive effect of choice history; humans: $\beta = 0.19 \pm$
²⁴ 1.4×10^{-4} , $z = 1.36 \times 10^3$, $p < 2.2 \times 10^{-308}$; mice: $\beta = 0.92 \pm 0.01$, $z = 88.82$, $p <$
²⁵ 2.2×10^{-308}). By contrast, perceptual choices tended to be repelled away from

26 the stimulus presented at preceding stimulus-incongruent trial (i.e., a negative
27 effect of stimulus history; humans: $\beta = -0.19 \pm 0.01$, $z = -16.47$, $p = 5.99 \times 10^{-61}$:
28 mice: $\beta = -0.92 \pm 0.01$, $z = -88.76$, $p < 2.2 \times 10^{-308}$). This repulsion of choices
29 away from stimuli presented at stimulus-incongruent trials confirmed that choices
30 (which are anti-correlated to stimuli at stimulus-incongruent trials) were the
31 primary driver of attracting serial effects in perception.

32 In sum, the above results suggest that, in both humans and mice, serial depen-
33 dencies were better explained by the effects of choice history as opposed to the
34 effects of stimulus history. This aligns with a result recently published for the
35 IBL database, where mice were shown to follow an *action-kernel* as opposed to a
36 *stimulus-kernel* model when integrating information across trials⁸¹.

37 1.2 Fluctuations between internal and external mode modulate 38 perceptual performance beyond the effect of general response 39 biases

40 The hypothesis that perception cycles through opposing internally- and externally-biased
41 modes is motivated by the assumption that recurring intervals of stronger perceptual history
42 temporally reduce the participants' sensitivity to external information. Importantly, the
43 history-dependent biases that characterize internal mode processing must be differentiated
44 from general response biases. In binary perceptual decision-making, general response biases
45 are defined by a propensity to choose one of the two outcomes more often than the alternative.
46 Indeed, human participants selected the more frequent of the two possible outcomes in 58.71%
47 $\pm 0.22\%$ of trials, and mice selected the more frequent of the two possible outcomes in 54.6%
48 $\pm 0.3\%$ of trials.

49 Two caveats have to be considered to make sure that the effect of history-congruence is
50 distinct from the effect of general response biases. First, history-congruent states become

51 more likely for larger response biases that cause an increasing imbalance in the likelihood of
52 the two outcomes (humans: $\beta = 0.24 \pm 6.93 \times 10^{-4}$, $T(2.09 \times 10^6) = 342.43$, $p < 2.2 \times 10^{-308}$;
53 mice: $\beta = 0.15 \pm 8.25 \times 10^{-4}$, $T(1.32 \times 10^6) = 181.93$, $p < 2.2 \times 10^{-308}$). One may thus
54 ask whether the autocorrelation of history-congruence could be entirely driven by general
55 response biases.

56 Importantly, our autocorrelation analyses account for general response biases by computing
57 group-level autocorrelations (Figure 2-4B) relative to randomly permuted data (i.e., by
58 subtracting the autocorrelation of randomly permuted data from the raw autocorrelation
59 curve). This precludes that general response biases contribute to the observed autocorrelation
60 of history-congruence (see Supplemental Figure S5 for a visualization of the correction
61 procedure for simulated data with general response biases ranging from 60 to 90%).

62 Second, it may be argued that fluctuations in perceptual performance may be solely driven
63 by ongoing changes in the strength of general response biases. To assess the links between
64 dynamic fluctuations in stimulus-congruence on the one hand and history-congruence as well
65 as general response bias on the other hand, we computed all variables as dynamic probabilities
66 in sliding windows of ± 5 trials (Figure 1C). Linear mixed effects modeling indicated that
67 fluctuations in history-congruent biases were larger in amplitude than the corresponding
68 fluctuations in general response biases in humans ($\beta_0 = 0.03 \pm 7.34 \times 10^{-3}$, $T(64.94) = 4.46$,
69 $p = 3.28 \times 10^{-5}$), but slightly smaller in mice ($\beta_0 = -5.26 \times 10^{-3} \pm 4.67 \times 10^{-4}$, $T(2.12 \times 10^3)$
70 $= -11.28$, $p = 1.02 \times 10^{-28}$).

71 Crucially, ongoing fluctuations in history-congruence had a significant negative effect on
72 stimulus-congruence (humans: $\beta_1 = -0.05 \pm 5.63 \times 10^{-4}$, $T(2.1 \times 10^6) = -84.21$, $p <$
73 2.2×10^{-308} ; mice: $\beta_1 = -0.12 \pm 7.17 \times 10^{-4}$, $T(1.34 \times 10^6) = -168.39$, $p < 2.2 \times 10^{-308}$)
74 beyond the effect of ongoing changes in general response biases (humans: $\beta_2 = -0.06 \pm$
75 5.82×10^{-4} , $T(2.1 \times 10^6) = -103.51$, $p < 2.2 \times 10^{-308}$; mice: $\beta_2 = -0.03 \pm 6.94 \times 10^{-4}$,
76 $T(1.34 \times 10^6) = -48.14$, $p < 2.2 \times 10^{-308}$). In sum, the above control analyses confirmed

77 that, in both humans and mice, the observed influence of preceding choices on perceptual
78 decision-making cannot be reduced to general response biases.

79 **1.3 Internal mode is characterized by lower thresholds as well as**
80 **by history-dependent changes in biases and lapses**

81 Random or stereotypical responses may provide an alternative explanation for the reduced
82 sensitivity to external sensory information that we attribute to internal mode processing. To
83 test this hypothesis, we asked whether history-independent changes in biases and lapses may
84 provide an alternative explanation of the reduced sensitivity during internal mode.

85 To this end, we estimated full and history-conditioned psychometric curves to investigate how
86 internal and external mode relate to biases (i.e., the horizontal position of the psychometric
87 curve), lapses (i.e., the asymptotes of the psychometric curve) and thresholds (i.e., 1/sensitivity,
88 estimated from the slope of the psychometric curve). We used a maximum likelihood procedure
89 to predict trial-wise choices y ($y = 0$ and $y = 1$ for outcomes A and B respectively) from
90 the choice probabilities y_p . y_p was computed from the difficulty-weighted inputs s_w via a
91 parametric error function defined by the parameters γ (lower lapse), δ (upper lapse), μ (bias)
92 and t (threshold; see Methods for details):

$$y_p = \gamma + (1 - \gamma - \delta) * (\text{erf}(\frac{s_w + \mu}{t}) + 1)/2 \quad (1)$$

93 Under our main hypothesis that periodic reductions in sensitivity to external information
94 are driven by increases in the impact of perceptual history, one would expect (i) a history-
95 dependent increase in biases and lapses (effects of perceptual history), and (ii), a history-
96 independent increase in threshold (reduced sensitivity to external information). Conversely,
97 if what we identified as internal mode processing was in fact driven by random choices, one
98 would expect (i), a history-independent increase in lapses (choice randomness), (ii), no change

99 in bias (no effect of perceptual history), and (iii), reduced thresholds (reduced sensitivity to
100 external information).

101 **1.3.1 Humans**

102 Across all data provided by the Confidence database²⁰ (i.e., irrespective of the preceding
103 perceptual choice y_{t-1}), biases μ were distributed around zero (-0.05 ± 0.03 ; $\beta_0 = 7.37 \times 10^{-3}$
104 ± 0.09 , $T(36.8) = 0.08$, $p = 0.94$; Supplemental Figure 6A-B, upper panel). When conditioned
105 on perceptual history, biases μ varied according to the preceding perceptual choice, with
106 negative biases for $y_{t-1} = 0$ (-0.22 ± 0.04 ; $\beta_0 = 0.56 \pm 0.12$, $T(43.39) = 4.6$, $p = 3.64 \times 10^{-5}$;
107 Supplemental Figure 6A-B, upper panel) and positive biases for $y_{t-1} = 1$ (0.29 ± 0.03 ; β_0
108 $= 0.56 \pm 0.12$, $T(43.39) = 4.6$, $p = 3.64 \times 10^{-5}$; Supplemental Figure 6A-B, lower panel).
109 Absolute biases $|\mu|$ were larger in internal mode (1.84 ± 0.03) as compared to external
110 mode (0.86 ± 0.02 ; $\beta_0 = -0.62 \pm 0.07$, $T(45.62) = -8.38$, $p = 8.59 \times 10^{-11}$; controlling for
111 differences in lapses and thresholds).

112 Lower and upper lapses amounted to $\gamma = 0.13 \pm 2.83 \times 10^{-3}$ and $\delta = 0.1 \pm 2.45 \times 10^{-3}$
113 (Supplemental Figure 6A, C and D). Lapses were larger in internal mode ($\gamma = 0.17 \pm$
114 3.52×10^{-3} , $\delta = 0.14 \pm 3.18 \times 10^{-3}$) as compared to external mode ($\gamma = 0.1 \pm 2.2 \times 10^{-3}$, $\delta =$
115 $0.08 \pm 2 \times 10^{-3}$; $\beta_0 = -0.05 \pm 5.73 \times 10^{-3}$, $T(47.03) = -9.11$, $p = 5.94 \times 10^{-12}$; controlling
116 for differences in biases and thresholds).

117 Conditioning on the previous perceptual choice revealed that the between-mode difference in
118 lapse was not general, but depended on perceptual history: For $y_{t-1} = 0$, only higher lapses δ
119 differed between internal and external mode ($\beta_0 = -0.1 \pm 9.58 \times 10^{-3}$, $T(36.87) = -10.16$, p
120 $= 3.06 \times 10^{-12}$), whereas lower lapses γ did not ($\beta_0 = 0.01 \pm 7.77 \times 10^{-3}$, $T(33.1) = 1.61$, p
121 $= 0.12$). Vice versa, for $y_{t-1} = 1$, lower lapses γ differed between internal and external mode
122 ($\beta_0 = -0.11 \pm 0.01$, $T(40.11) = -9.59$, $p = 6.14 \times 10^{-12}$), whereas higher lapses δ did not
123 ($\beta_0 = 0.01 \pm 7.74 \times 10^{-3}$, $T(33.66) = 1.58$, $p = 0.12$).

₁₂₄ Thresholds t were estimated at 3 ± 0.06 (Supplemental Figure 6A and E). Thresholds t were
₁₂₅ larger in internal mode (3.66 ± 0.09) as compared to external mode (2.02 ± 0.03 ; $\beta_0 = -1.77$
₁₂₆ ± 0.25 , $T(50.45) = -7.14$, $p = 3.48 \times 10^{-9}$; controlling for differences in biases and lapses).
₁₂₇ In contrast to the bias μ and the lapse rates γ and δ , thresholds t were not modulated by
₁₂₈ perceptual history ($\beta_0 = 0.04 \pm 0.06$, $T(2.97 \times 10^3) = 0.73$, $p = 0.47$).

₁₂₉ **1.3.2 Mice**

₁₃₀ When estimated based on the full dataset provided in the IBL database²¹ (i.e., irrespective
₁₃₁ of the preceding perceptual choice y_{t-1}), biases μ were distributed around zero (3.87×10^{-3}
₁₃₂ $\pm 9.81 \times 10^{-3}$; $T(164) = 0.39$, $p = 0.69$; Supplemental Figure 7A-B, upper panel). When
₁₃₃ conditioned on the preceding perceptual choice, biases were negative for $y_{t-1} = 0$ (-0.02
₁₃₄ $\pm 8.7 \times 10^{-3}$; $T(164) = -1.99$, $p = 0.05$; Supplemental Figure 7A-B, middle panel) and
₁₃₅ positive for $y_{t-1} = 1$ ($0.02 \pm 9.63 \times 10^{-3}$; $T(164) = 1.91$, $p = 0.06$; Supplemental Figure
₁₃₆ 7A-B, lower panel). As in humans, mice showed larger biases during internal mode (0.14
₁₃₇ $\pm 7.96 \times 10^{-3}$) as compared to external mode ($0.07 \pm 8.7 \times 10^{-3}$; $\beta_0 = -0.18 \pm 0.03$, $T =$
₁₃₈ -6.38 , $p = 1.77 \times 10^{-9}$; controlling for differences in lapses and thresholds).

₁₃₉ Lower and upper lapses amounted to $\gamma = 0.1 \pm 4.35 \times 10^{-3}$ and $\delta = 0.11 \pm 4.65 \times 10^{-3}$
₁₄₀ (Supplemental Figure 7A, C and D). Lapse rates were higher in internal mode ($\gamma = 0.15 \pm$
₁₄₁ 5.14×10^{-3} , $\delta = 0.16 \pm 5.79 \times 10^{-3}$) as compared to external mode ($\gamma = 0.06 \pm 3.11 \times 10^{-3}$,
₁₄₂ $\delta = 0.07 \pm 3.34 \times 10^{-3}$; $\beta_0 = -0.11 \pm 4.39 \times 10^{-3}$, $T = -24.8$, $p = 4.91 \times 10^{-57}$; controlling
₁₄₃ for differences in biases and thresholds).

₁₄₄ For $y_{t-1} = 0$, the difference between internal and external mode was more pronounced for
₁₄₅ higher lapses δ ($T(164) = 21.44$, $p = 1.93 \times 10^{-49}$). Conversely, for $y_{t-1} = 1$, the difference
₁₄₆ between internal and external mode was more pronounced for lower lapses γ ($T(164) =$
₁₄₇ -18.24 , $p = 2.68 \times 10^{-41}$). In contrast to the human data, higher lapses δ and lower lapses
₁₄₈ γ were significantly elevated during internal mode irrespective of the preceding perceptual
₁₄₉ choice (higher lapses δ for $y_{t-1} = 1$: $T(164) = -2.65$, $p = 8.91 \times 10^{-3}$; higher lapses δ for

₁₅₀ $y_{t-1} = 0$: $T(164) = -28.29$, $p = 5.62 \times 10^{-65}$; lower lapses γ for $y_{t-1} = 1$: $T(164) = -32.44$, p
₁₅₁ $= 2.92 \times 10^{-73}$; lower lapses γ for $y_{t-1} = 0$: $T(164) = -2.5$, $p = 0.01$.

₁₅₂ In mice, thresholds t amounted to $0.15 \pm 6.52 \times 10^{-3}$ (Supplemental Figure 7A and E) and
₁₅₃ were higher in internal mode (0.27 ± 0.01) as compared to external mode ($0.09 \pm 4.44 \times 10^{-3}$;
₁₅₄ $\beta_0 = -0.28 \pm 0.04$, $T = -7.26$, $p = 1.53 \times 10^{-11}$; controlling for differences in biases and
₁₅₅ lapses). Thresholds t were not modulated by perceptual history ($T(164) = 0.94$, $p = 0.35$).

₁₅₆ In sum, the above analyses showed that, in both humans and mice, internal and external
₁₅₇ mode differ with respect to biases, lapses and thresholds. Internally-biased processing was
₁₅₈ characterized by higher thresholds, indicating a reduced sensitivity to sensory information,
₁₅₉ as well as by larger biases and lapses. Importantly, between-mode differences in biases and
₁₆₀ lapses strongly depended on perceptual history. This confirmed that internal mode processing
₁₆₁ cannot be explained solely on the ground of a general (i.e., history-independent) increase in
₁₆₂ lapses or bias indicative of random or stereotypical responses.

₁₆₃ **1.4 Internal mode processing can not be reduced to insufficient 164 task familiarity**

₁₆₅ It may be assumed that participants tend to repeat preceding choices when they are not yet
₁₆₆ familiar with the experimental task, leading to history-congruent choices that are caused by
₁₆₇ insufficient training. To assess this alternative explanation, we contrasted the correlates of
₁₆₈ bimodal inference with training effects in humans and mice.

₁₆₉ **1.4.1 Humans**

₁₇₀ In the Confidence database²⁰, training effects were visible from RTs that were shortened by
₁₇₁ increasing exposure to the task ($\beta = -7.53 \times 10^{-5} \pm 6.32 \times 10^{-7}$, $T(1.81 \times 10^6) = -119.15$, p
₁₇₂ $< 2.2 \times 10^{-308}$). Intriguingly, however, history-congruent choices became more frequent with
₁₇₃ increased exposure to the task ($\beta = 3.6 \times 10^{-5} \pm 2.54 \times 10^{-6}$, $z = 14.19$, $p = 10^{-45}$), speaking

¹⁷⁴ against the proposition that insufficient training induces seriality in response behavior.

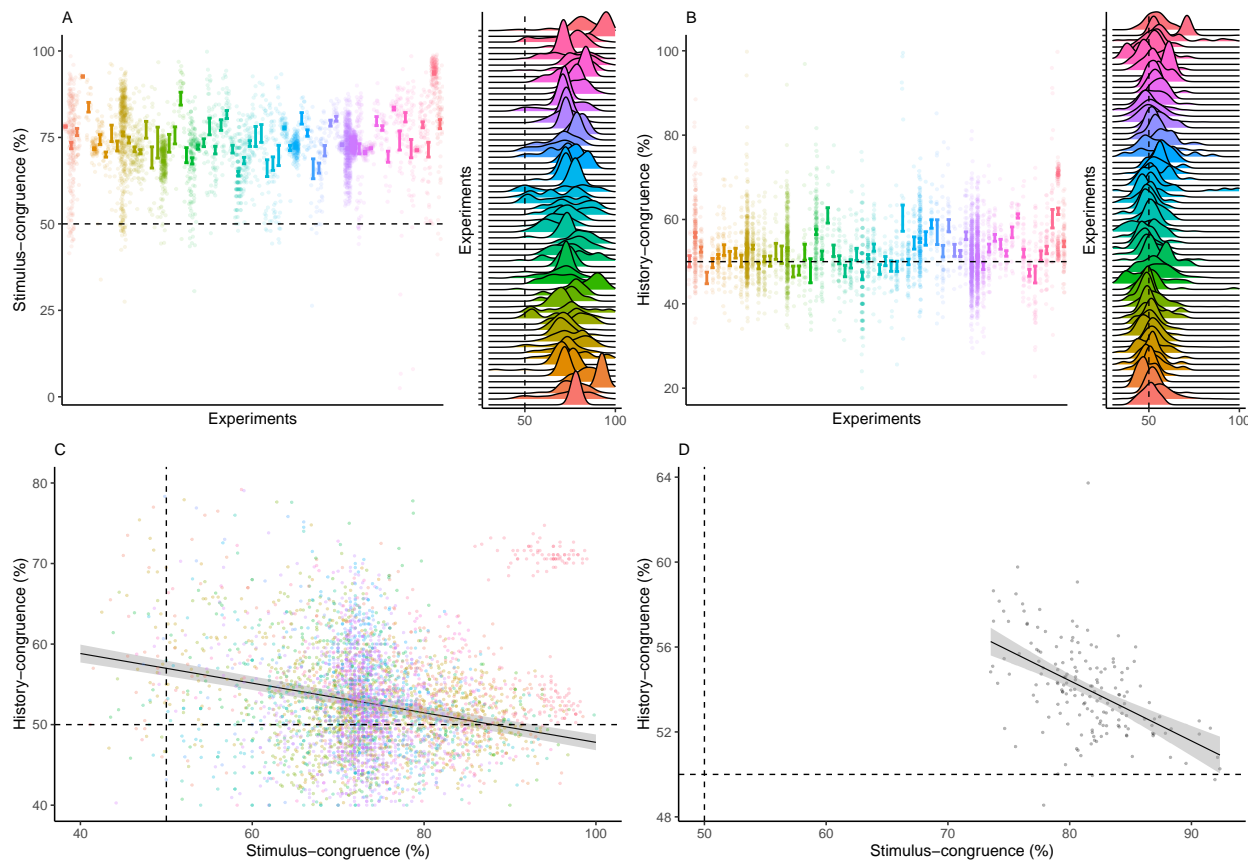
¹⁷⁵ **1.4.2 Mice**

¹⁷⁶ As in humans, it is an important caveat to consider whether the observed serial dependencies
¹⁷⁷ in mice reflect a phenomenon of perceptual inference, or, alternatively, an unspecific strategy
¹⁷⁸ that occurs at the level of reporting behavior. We reasoned that, if mice indeed tended to
¹⁷⁹ repeat previous choices as a general response pattern, history effects should decrease during
¹⁸⁰ training of the perceptual task. We therefore analyzed how stimulus- and history-congruent
¹⁸¹ perceptual choices evolved across sessions in mice that, by the end of training, achieved
¹⁸² proficiency (i.e., stimulus-congruence $\geq 80\%$) in the *basic* task of the IBL dataset²¹.

¹⁸³ Across sessions, we found that stimulus-congruent perceptual choices became more frequent
¹⁸⁴ ($\beta = 0.34 \pm 7.13 \times 10^{-3}$, $T(8.51 \times 10^3) = 47.66$, $p < 2.2 \times 10^{-308}$) and TDs were progressively
¹⁸⁵ shortened ($\beta = -22.14 \pm 17.06$, $T(1.14 \times 10^3) = -1.3$, $p < 2.2 \times 10^{-308}$). Crucially, the
¹⁸⁶ frequency of history-congruent perceptual choices also increased during training ($\beta = 0.13 \pm$
¹⁸⁷ 4.67×10^{-3} , $T(8.4 \times 10^3) = 27.04$, $p = 1.96 \times 10^{-154}$; Supplemental Figure S8).

¹⁸⁸ Within individual session, longer task exposure was associated with an increase in history-
¹⁸⁹ congruence ($\beta = 3.6 \times 10^{-5} \pm 2.54 \times 10^{-6}$, $z = 14.19$, $p = 10^{-45}$) and a decrease in TDs (β
¹⁹⁰ $= -0.1 \pm 3.96 \times 10^{-3}$, $T(1.34 \times 10^6) = -24.99$, $p = 9.45 \times 10^{-138}$). In sum, these findings
¹⁹¹ strongly argue against the proposition that mice show biases toward perceptual history due
¹⁹² to an unspecific response strategy.

193 **1.5 Supplemental Figure S1**



194

195 **Supplemental Figure S1. Stimulus- and history-congruence.**

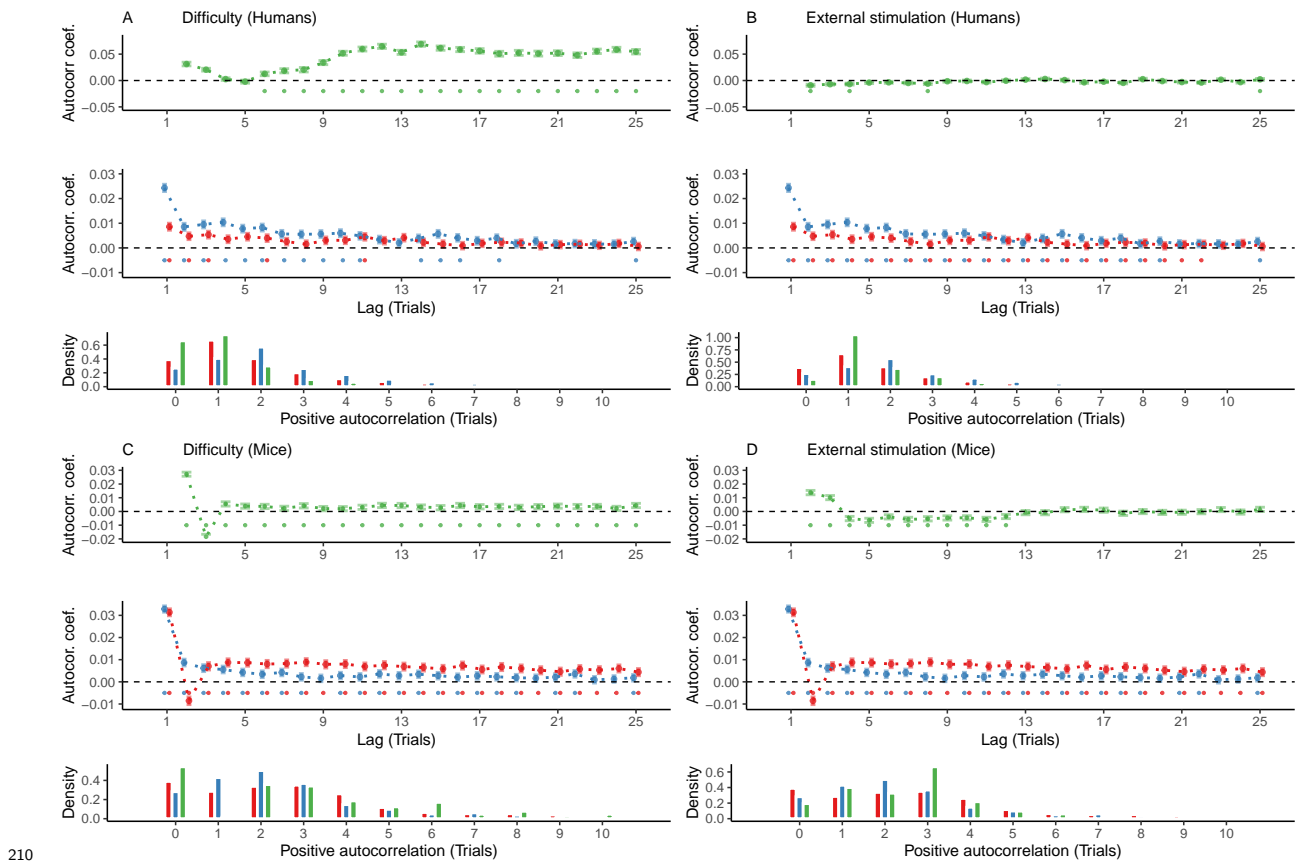
196 A. Stimulus-congruent choices in humans amounted to $73.46\% \pm 0.15\%$ of trials and were
197 highly consistent across the experiments selected from the Confidence Database.

198 B. History-congruent choices in humans amounted to $52.7\% \pm 0.12\%$ of trials. In analogy
199 to stimulus-congruence, the prevalence of history-congruence was highly consistent across
200 the experiments selected from the Confidence Database. 48.48% of experiments showed
201 significant ($p < 0.05$) biases toward preceding choices, whereas 2 of the 66 of the included
202 experiments showed significant repelling biases.

203 C. In humans, we found an enhanced impact of perceptual history in participants who were
204 less sensitive to external sensory information ($T(4.3 \times 10^3) = -14.27$, $p = 3.78 \times 10^{-45}$),
205 suggesting that perception results from the competition of external with internal information.

²⁰⁶ D. In analogy to humans, mice that were less sensitive to external sensory information
²⁰⁷ showed stronger biases toward perceptual history ($T(163) = -7.52$, $p = 3.44 \times 10^{-12}$, Pearson
²⁰⁸ correlation).

209 **1.6 Supplemental Figure S2**



210 **211 Supplemental Figure S2. Controlling for task difficulty and external stimulation.**

212 In this study, we found highly significant autocorrelations of stimulus- and history-congruence
 213 in humans as well as in mice, while controlling for task difficulty and the sequence of external
 214 stimulation. **Here, we confirm that the autocorrelations of stimulus- and history-**
 215 **congruence were not a trivial consequence of the experimental design or the**
 216 **addition of task difficulty and external stimulation as control variables in the**
 217 **computation of group-level autocorrelations.**

218 A. In humans, task difficulty (in green) showed a significant autocorrelation starting at the
 219 5th trial (upper panel, dots at the bottom indicate intercepts $\neq 0$ in trial-wise linear mixed
 220 effects modeling at $p < 0.05$). When controlling for task difficulty only, linear mixed effects
 221 modeling indicated a significant autocorrelation of stimulus-congruence (in red) for the first 3
 222 consecutive trials (middle panel). 20% of trials within the displayed time window remained

223 significantly autocorrelated. The autocorrelation of history-congruence (in blue) remained
224 significant for the first 11 consecutive trials (64% significantly autocorrelated trials within
225 the displayed time window). At the level of individual participants, the autocorrelation of
226 task difficulty exceeded the respective autocorrelation of randomly permuted within a lag of
227 $21.66 \pm 8.37 \times 10^{-3}$ trials (lower panel).

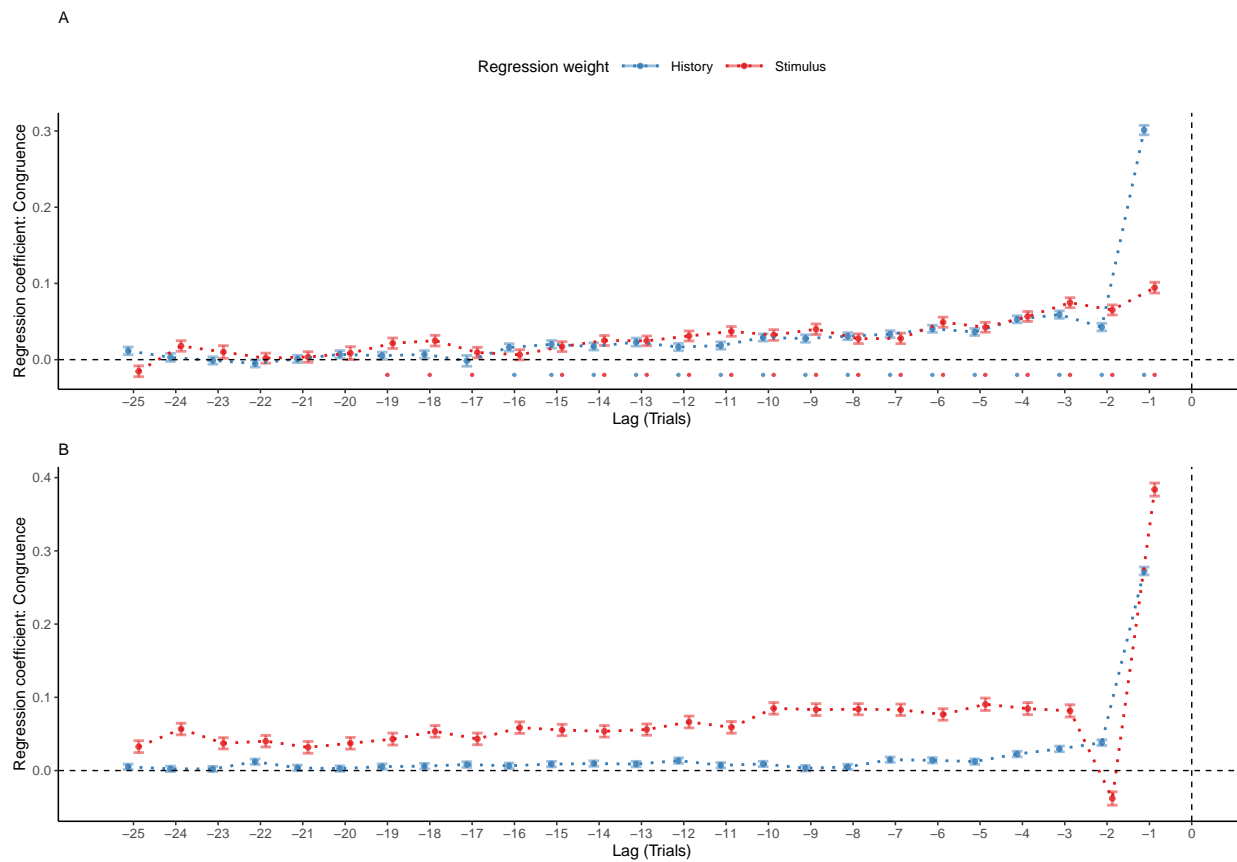
228 B. In humans, the sequence of external stimulation (i.e., which of the two binary outcomes
229 was supported by the presented stimuli; depicted in green) was negatively autocorrelated
230 for 1 trial. When controlling for the autocorrelation of external stimulation only, stimulus-
231 congruence remained significantly autocorrelated for 22 consecutive trials (88% of trials
232 within the displayed time window; lower panel) and history-congruence remained significantly
233 autocorrelated for 20 consecutive trials (84% of trials within the displayed time window). At
234 the level of individual participants, the autocorrelation of external stimulation exceeded the
235 respective autocorrelation of randomly permuted within a lag of $2.94 \pm 4.4 \times 10^{-3}$ consecutive
236 trials (lower panel).

237 C. In mice, task difficulty showed a significant autocorrelated for the first 25 consecutive trials
238 (upper panel). When controlling only for task difficulty only, linear mixed effects modeling
239 indicated a significant autocorrelation of stimulus-congruence for the first 36 consecutive trials
240 (middle panel). In total, 100% of trials within the displayed time window remained significantly
241 autocorrelated. The autocorrelation of history-congruence remained significant for the first
242 8 consecutive trials, with 84% significantly autocorrelated trials within the displayed time
243 window. At the level of individual mice, autocorrelation coefficients for difficulty were elevated
244 above randomly permuted data within a lag of 15.13 ± 0.19 consecutive trials (lower panel).

245 D. In mice, the sequence of external stimulation (i.e., which of the two binary outcomes was
246 supported by the presented stimuli) was negatively autocorrelated for 11 consecutive trials
247 (upper panel). When controlling only for the autocorrelation of external stimulation, stimulus-
248 congruence remained significantly autocorrelated for 86 consecutive trials (100% of trials

²⁴⁹ within the displayed time window; middle) and history-congruence remained significantly
²⁵⁰ autocorrelated for 8 consecutive trials (84% of trials within the displayed time window). At
²⁵¹ the level of individual mice, autocorrelation coefficients for external stimulation were elevated
²⁵² above randomly permuted data within a lag of $2.53 \pm 9.8 \times 10^{-3}$ consecutive trials (lower
²⁵³ panel).

254 **1.7 Supplemental Figure S3**



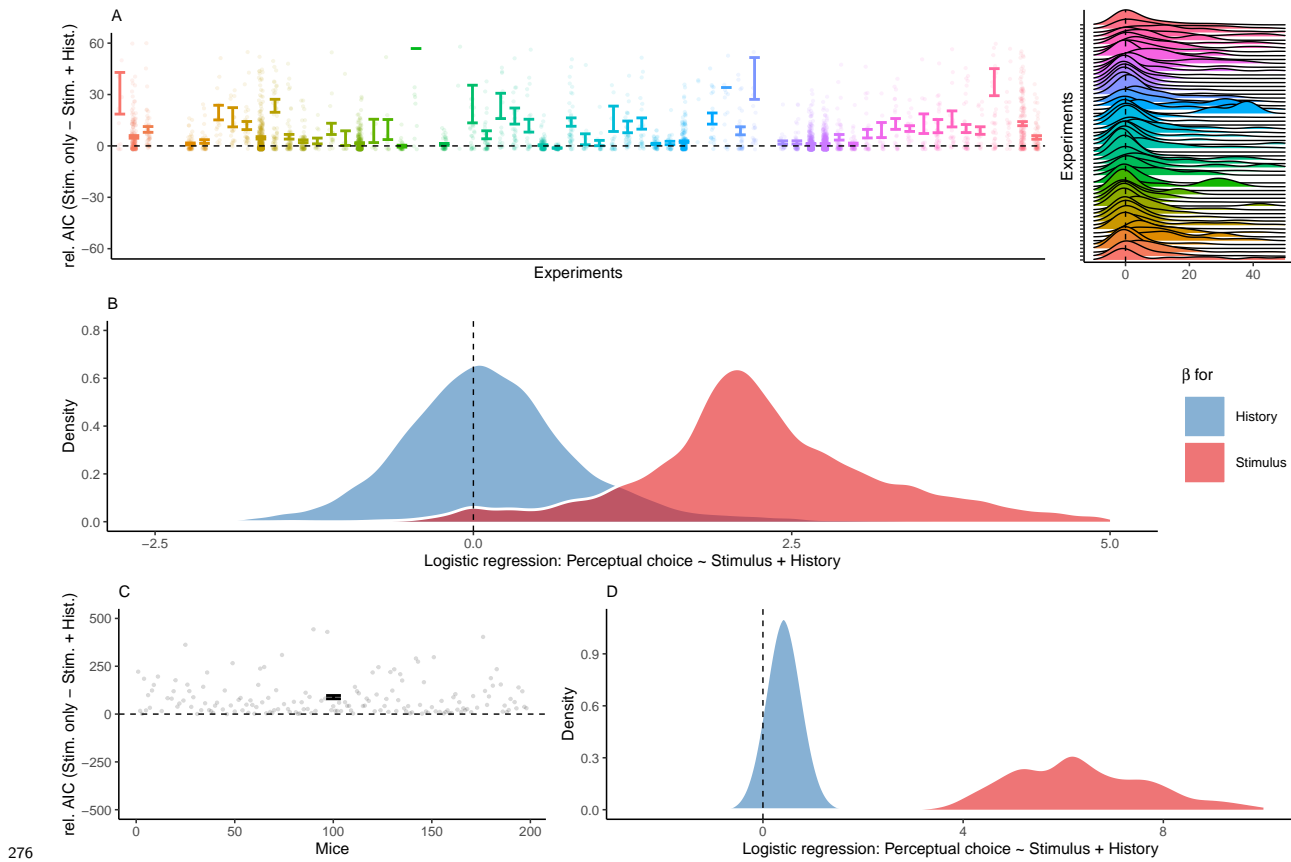
255
 256 **Supplemental Figure S3. Reproducing group-level autocorrelations using logistic**
 257 **regression.**

258 A. As an alternative to group-level autocorrelation coefficients, we used trial-wise logistic
 259 regression to quantify serial dependencies in stimulus- and history-congruence. This analysis
 260 predicted stimulus- and history-congruence at the index trial (trial $t = 0$, vertical line) based
 261 on stimulus- and history-congruence at the 100 preceding trials. Mirroring the shape of the
 262 group-level autocorrelations, trial-wise regression coefficients (depicted as mean \pm SEM, dots
 263 mark trials with regression weights significantly greater than zero at $p < 0.05$) increased
 264 toward the index trial $t = 0$ for the human data.

265 B. Following our results in human data, regression coefficients that predicted history-
 266 congruence at the index trial (trial $t = 0$, vertical line) increased exponentially for trials
 267 closer to the index trial in mice. In contrast to history-congruence, stimulus-congruence

²⁶⁸ showed a negative regression weight (or autocorrelation coefficient; Figure 3B) at trial -2.
²⁶⁹ This was due to the experimental design (see also the autocorrelations of difficulty and
²⁷⁰ external stimulation in Supplemental Figure S2C and D): When mice made errors at easy
²⁷¹ trials (contrast $\geq 50\%$), the upcoming stimulus was shown at the same spatial location and at
²⁷² high contrast. This increased the probability of stimulus-congruent perceptual choices after
²⁷³ stimulus-incongruent perceptual choices at easy trials, thereby creating a negative regression
²⁷⁴ weight (or autocorrelation coefficient) of stimulus-congruence at trial -2.

275 **1.8 Supplemental Figure S4**



276 **277 Supplemental Figure S4. History-congruence in logistic regression.**

278 A. To ensure that perceptual history played a significant role in perception despite the ongoing
 279 stream of external information, we tested whether human perceptual decision-making was
 280 better explained by the combination of external and internal information or, alternatively,
 281 by external information alone. To this end, we compared AIC between logistic regression
 282 models that predicted trial-wise perceptual responses either by both current external sensory
 283 information and the preceding percept, or by external sensory information alone (values above
 284 zero indicate a superiority of the full model). With high consistency across the experiments
 285 selected from the Confidence Database, this model-comparison confirmed that perceptual
 286 history contributed significantly to perception (difference in AIC = 8.07 ± 0.53 , $T(57.22) =$
 287 4.1 , $p = 1.31 \times 10^{-4}$).

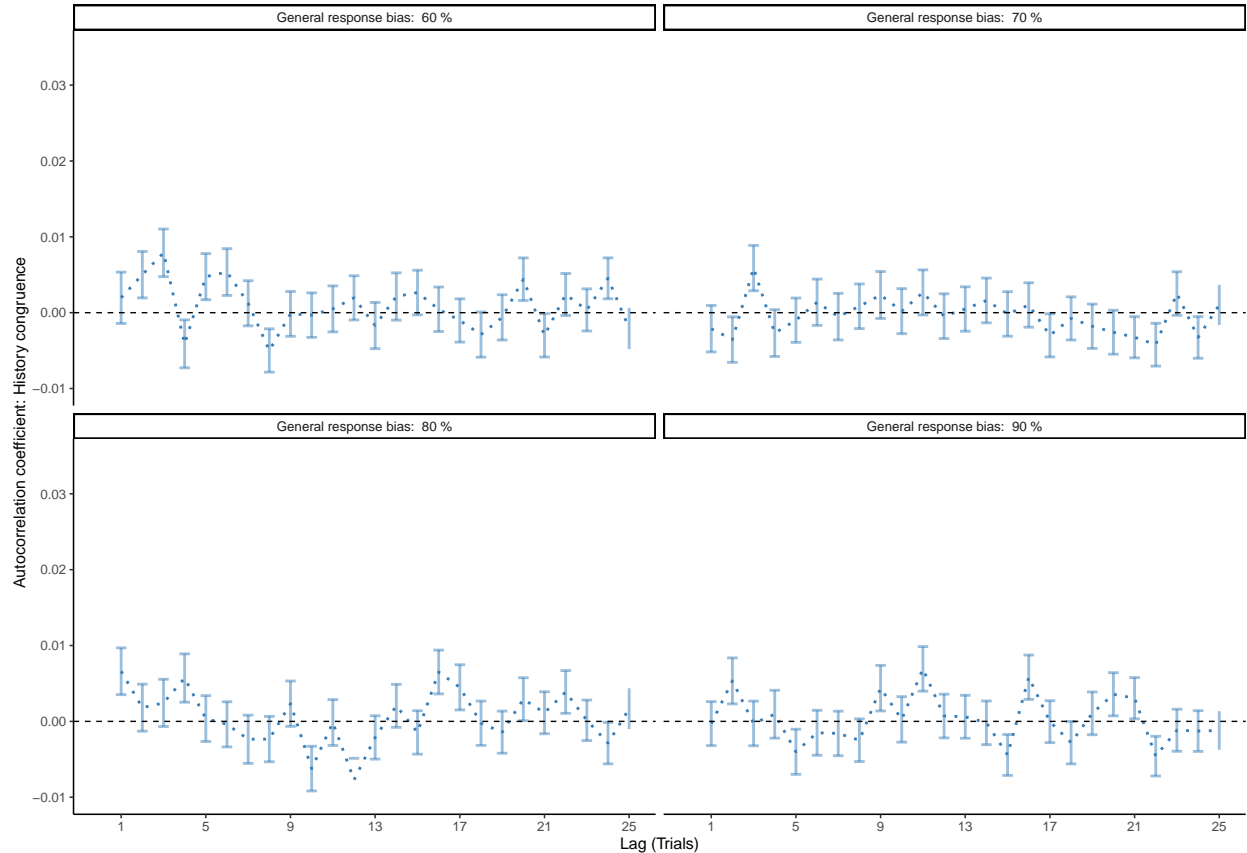
288 B. Participant-wise regression coefficients amount to 0.18 ± 0.02 for the effect of perceptual

²⁸⁹ history and 2.51 ± 0.03 for external sensory stimulation.

²⁹⁰ C. In mice, an AIC-based model comparison indicated that perception was better explained
²⁹¹ by logistic regression models that predicted trial-wise perceptual responses based on both
²⁹² current external sensory information and the preceding percept (difference in AIC = $88.62 \pm$
²⁹³ 8.57 , $T(164) = -10.34$, $p = 1.29 \times 10^{-19}$).

²⁹⁴ D. In mice, individual regression coefficients amounted to 0.42 ± 0.02 for the effect of
²⁹⁵ perceptual history and 6.91 ± 0.21 for external sensory stimulation.

296 **1.9 Supplemental Figure S5**



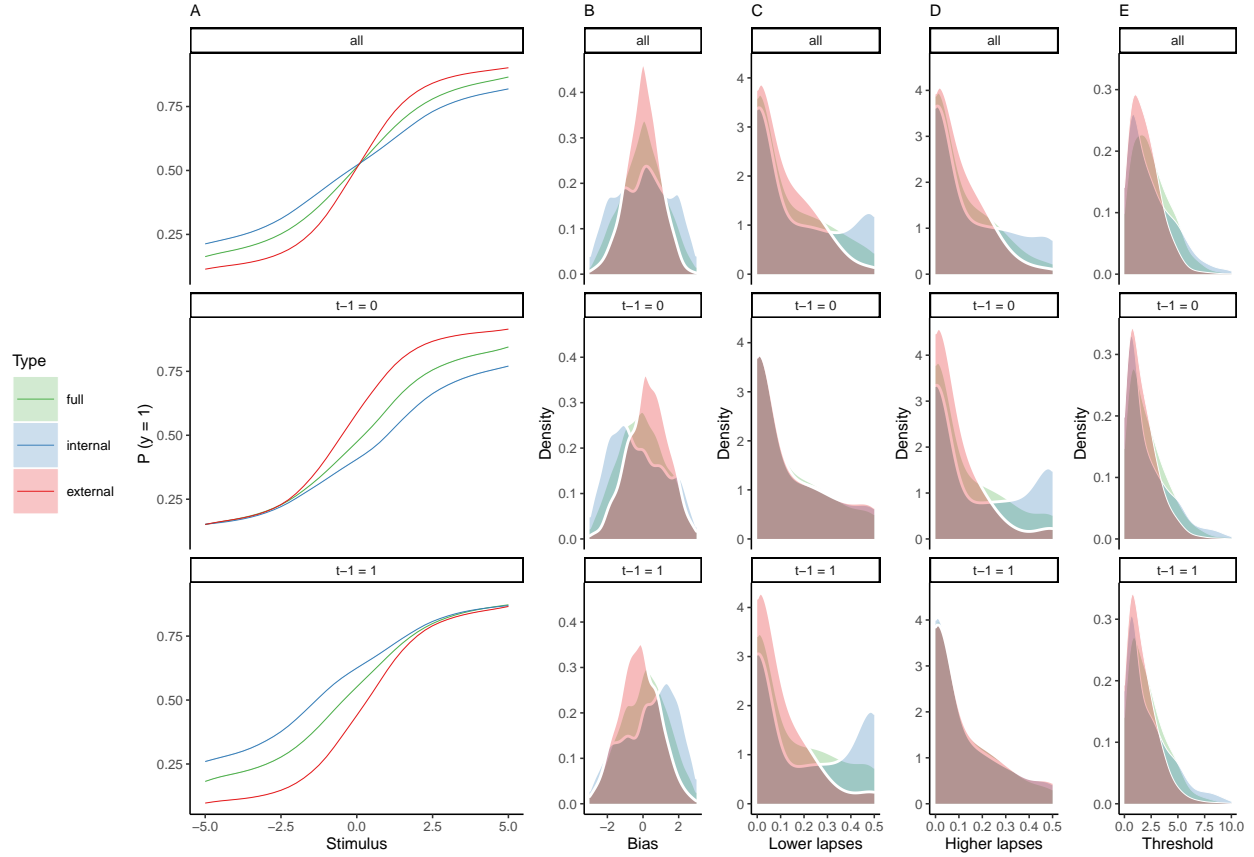
297

298 **Supplemental Figure S5. Correcting for general response biases.**

299 Here, we ask whether the autocorrelation of history-congruence (as shown in Figure 2-3C)
300 may be driven by general response biases (i.e., a general propensity to choose one of the two
301 possible outcomes more frequently than the alternative). To this end, we generated sequences
302 of 100 perceptual choices with general response biases ranging from 60 to 90% for 1000
303 simulated participants each. We then computed the autocorrelation of history-congruence
304 for these simulated data. Crucially, we used the correction procedure that is applied to the
305 autocorrelation curves shown in this manuscript: All reported autocorrelation coefficients are
306 computed relative to the average autocorrelation coefficients obtained for 100 iterations of
307 randomly permuted trial sequences. The above simulation show that this correction procedure
308 removes any potential contribution of general response biases to the autocorrelation of history-
309 congruence. This indicates that the autocorrelation of history-congruence (as shown in Figure

₃₁₀ 2-3C) is not driven by general response biases that were present in the empirical data at a
₃₁₁ level of $58.71\% \pm 0.22\%$ in humans and $54.6\% \pm 0.3\%$ in mice.

312 **1.10 Supplemental Figure S6**



313 **314 Supplemental Figure S6. Full and history-conditioned psychometric functions**

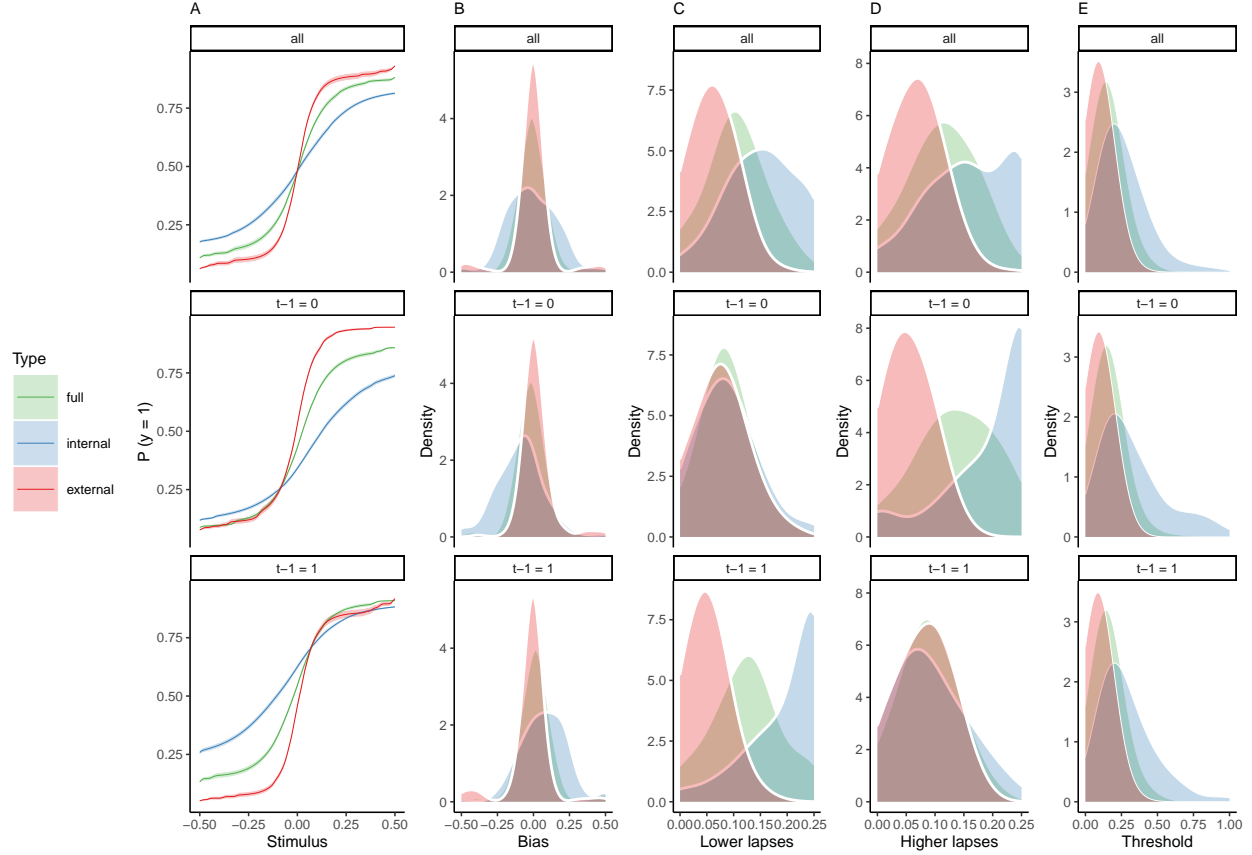
315 **across modes in humans.**

316 A. Here, we show average psychometric functions for the full dataset (upper panel) and
 317 conditioned on perceptual history ($y_{t-1} = 1$ and $y_{t-1} = 0$; middle and lower panel) across
 318 modes (green line) and for internal mode (blue line) and external mode (red line) separately.

319 B. Across the full dataset, biases μ were distributed around zero ($\beta_0 = 7.37 \times 10^{-3} \pm 0.09$,
 320 $T(36.8) = 0.08$, $p = 0.94$; upper panel), with larger absolute biases $|\mu|$ for internal as compared
 321 to external mode ($\beta_0 = -0.62 \pm 0.07$, $T(45.62) = -8.38$, $p = 8.59 \times 10^{-11}$; controlling for
 322 differences in lapses and thresholds). When conditioned on perceptual history, we observed
 323 negative biases for $y_{t-1} = 0$ ($\beta_0 = 0.56 \pm 0.12$, $T(43.39) = 4.6$, $p = 3.64 \times 10^{-5}$; middle
 324 panel) and positive biases for $y_{t-1} = 1$ ($\beta_0 = 0.56 \pm 0.12$, $T(43.39) = 4.6$, $p = 3.64 \times 10^{-5}$;
 325 lower panel).

- 326 C. Lapse rates were higher in internal mode as compared to external mode ($\beta_0 = -0.05 \pm$
327 5.73×10^{-3} , $T(47.03) = -9.11$, $p = 5.94 \times 10^{-12}$; controlling for differences in biases and
328 thresholds; see upper panel and subplot D). Importantly, the between-mode difference in
329 lapses depended on perceptual history: We found no significant difference in lower lapses
330 γ for $y_{t-1} = 0$ ($\beta_0 = 0.01 \pm 7.77 \times 10^{-3}$, $T(33.1) = 1.61$, $p = 0.12$; middle panel), but a
331 significant difference for $y_{t-1} = 1$ ($\beta_0 = -0.11 \pm 0.01$, $T(40.11) = -9.59$, $p = 6.14 \times 10^{-12}$;
332 lower panel).
- 333 D. Conversely, higher lapses δ were significantly increased for $y_{t-1} = 0$ ($\beta_0 = -0.1 \pm$
334 9.58×10^{-3} , $T(36.87) = -10.16$, $p = 3.06 \times 10^{-12}$; middle panel), but not for $y_{t-1} = 1$ ($\beta_0 =$
335 $0.01 \pm 7.74 \times 10^{-3}$, $T(33.66) = 1.58$, $p = 0.12$; lower panel).
- 336 E. The thresholds t were larger in internal as compared to external mode ($\beta_0 = -1.77 \pm 0.25$,
337 $T(50.45) = -7.14$, $p = 3.48 \times 10^{-9}$; controlling for differences in biases and lapses) and were
338 not modulated by perceptual history ($\beta_0 = 0.04 \pm 0.06$, $T(2.97 \times 10^3) = 0.73$, $p = 0.47$).

339 **1.11 Supplemental Figure S7**



340 **341 Supplemental Figure S7. Full and history-conditioned psychometric functions**

342 across modes in mice.

343 A. Here, we show average psychometric functions for the full IBL dataset (upper panel) and
344 conditioned on perceptual history ($y_{t-1} = 1$ and $y_{t-1} = 0$; middle and lower panel) across
345 modes (green line) and for internal mode (blue line) and external mode (red line) separately.

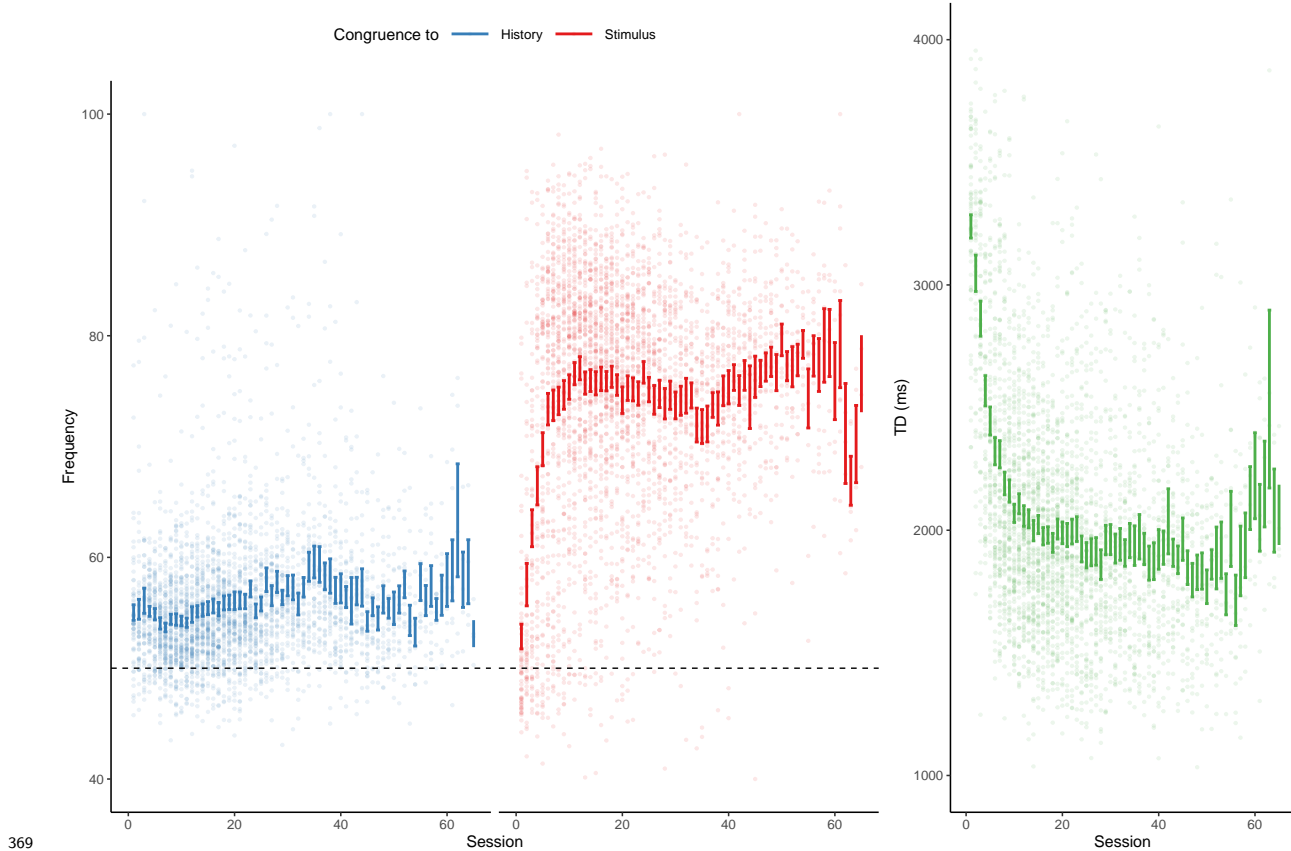
346 B. Across the full dataset, biases μ were distributed around zero ($T(164) = 0.39$, $p = 0.69$;
347 upper panel), with larger absolute biases $|\mu|$ for internal as compared to external mode ($\beta_0 =$
348 -0.18 ± 0.03 , $T = -6.38$, $p = 1.77 \times 10^{-9}$; controlling for differences in lapses and thresholds).
349 When conditioned on perceptual history, we observed negative biases for $y_{t-1} = 0$ ($T(164)$
350 $= -1.99$, $p = 0.05$; middle panel) and positive biases for $y_{t-1} = 1$ ($T(164) = 1.91$, $p = 0.06$;
351 lower panel).

³⁵² C. Lapse rates were higher in internal as compared to external mode ($\beta_0 = -0.11 \pm 4.39 \times 10^{-3}$,
³⁵³ $T = -24.8$, $p = 4.91 \times 10^{-57}$; controlling for differences in biases and thresholds; upper
³⁵⁴ panel, see subplot D). For $y_{t-1} = 1$, the difference between internal and external mode was
³⁵⁵ more pronounced for lower lapses γ ($T(164) = -18.24$, $p = 2.68 \times 10^{-41}$) as compared to
³⁵⁶ higher lapses δ (see subplot D). In mice, lower lapses γ were significantly elevated during
³⁵⁷ internal mode irrespective of the preceding perceptual choice (middle panel: lower lapses γ
³⁵⁸ for $y_{t-1} = 0$; $T(164) = -2.5$, $p = 0.01$, lower panel: lower lapses γ for $y_{t-1} = 1$; $T(164) =$
³⁵⁹ -32.44 , $p = 2.92 \times 10^{-73}$).

³⁶⁰ D. For $y_{t-1} = 0$, the difference between internal and external mode was more pronounced
³⁶¹ for higher lapses δ ($T(164) = 21.44$, $p = 1.93 \times 10^{-49}$, see subplot C). Higher lapses were
³⁶² significantly elevated during internal mode irrespective of the preceding perceptual choice
³⁶³ (middle panel: higher lapses δ for $y_{t-1} = 0$; $T(164) = -28.29$, $p = 5.62 \times 10^{-65}$ lower panel:
³⁶⁴ higher lapses δ for $y_{t-1} = 1$; $T(164) = -2.65$, $p = 8.91 \times 10^{-3}$;).

³⁶⁵ E. Thresholds t were higher in internal as compared to external mode ($\beta_0 = -0.28 \pm 0.04$,
³⁶⁶ $T = -7.26$, $p = 1.53 \times 10^{-11}$; controlling for differences in biases and lapses) and were not
³⁶⁷ modulated by perceptual history ($T(164) = 0.94$, $p = 0.35$).

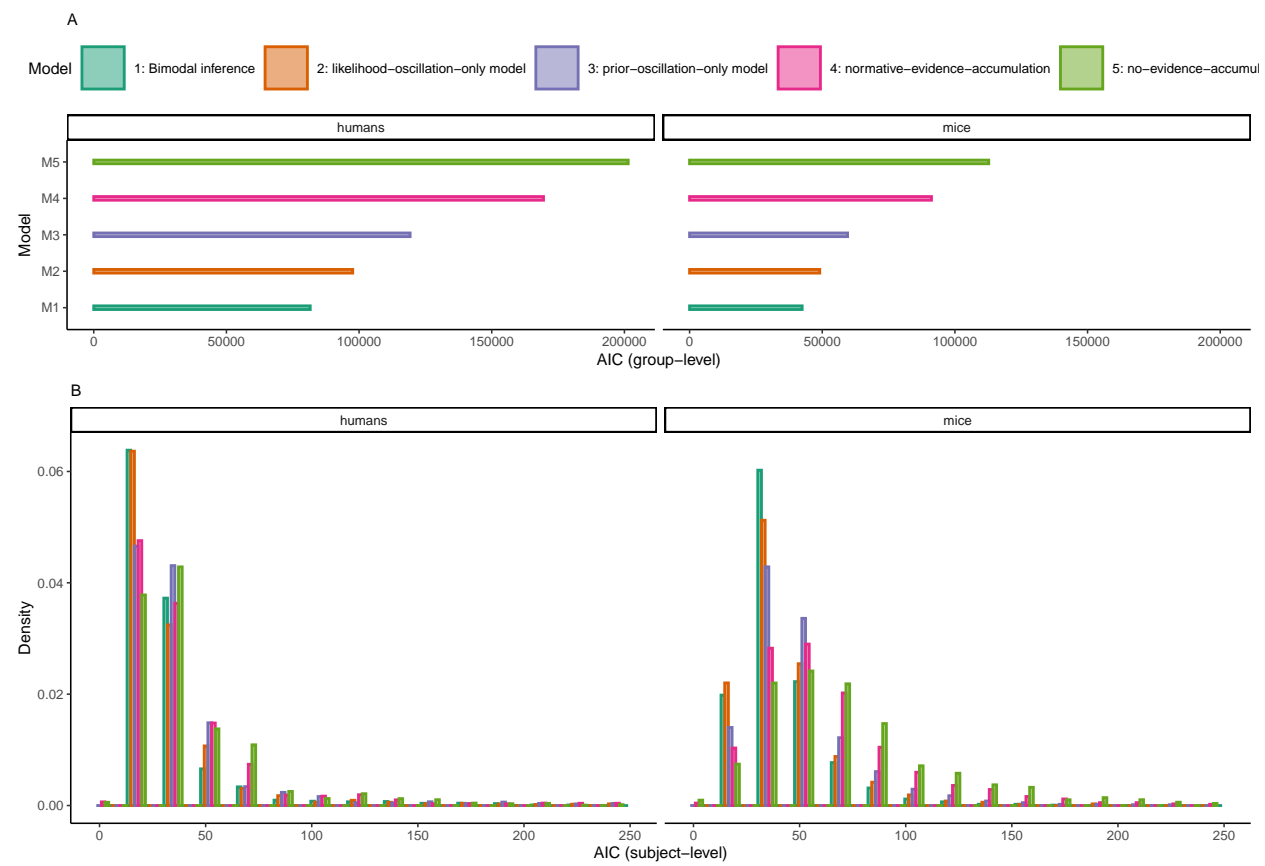
³⁶⁸ **1.12 Supplemental Figure S8**



³⁷⁰ **Supplemental Figure S8. History-/stimulus-congruence and TDs during training
371 of the basic task.**

³⁷² Here, we depict the progression of history- and stimulus-congruence (depicted in blue and
373 red, respectively; left panel) as well as TDs (in green; right panel) across training sessions in
374 mice that achieved proficiency (i.e., stimulus-congruence $\geq 80\%$) in the *basic* task of the IBL
375 dataset. We found that both history-congruent perceptual choices ($\beta = 0.13 \pm 4.67 \times 10^{-3}$,
376 $T(8.4 \times 10^3) = 27.04$, $p = 1.96 \times 10^{-154}$) and stimulus-congruent perceptual choices ($\beta =$
377 $0.34 \pm 7.13 \times 10^{-3}$, $T(8.51 \times 10^3) = 47.66$, $p < 2.2 \times 10^{-308}$) became more frequent with
378 training. As in humans, mice showed shorter TDs with increased exposure to the task ($\beta =$
379 -22.14 ± 17.06 , $T(1.14 \times 10^3) = -1.3$, $p < 2.2 \times 10^{-308}$).

380 **1.13 Supplemental Figure S9**



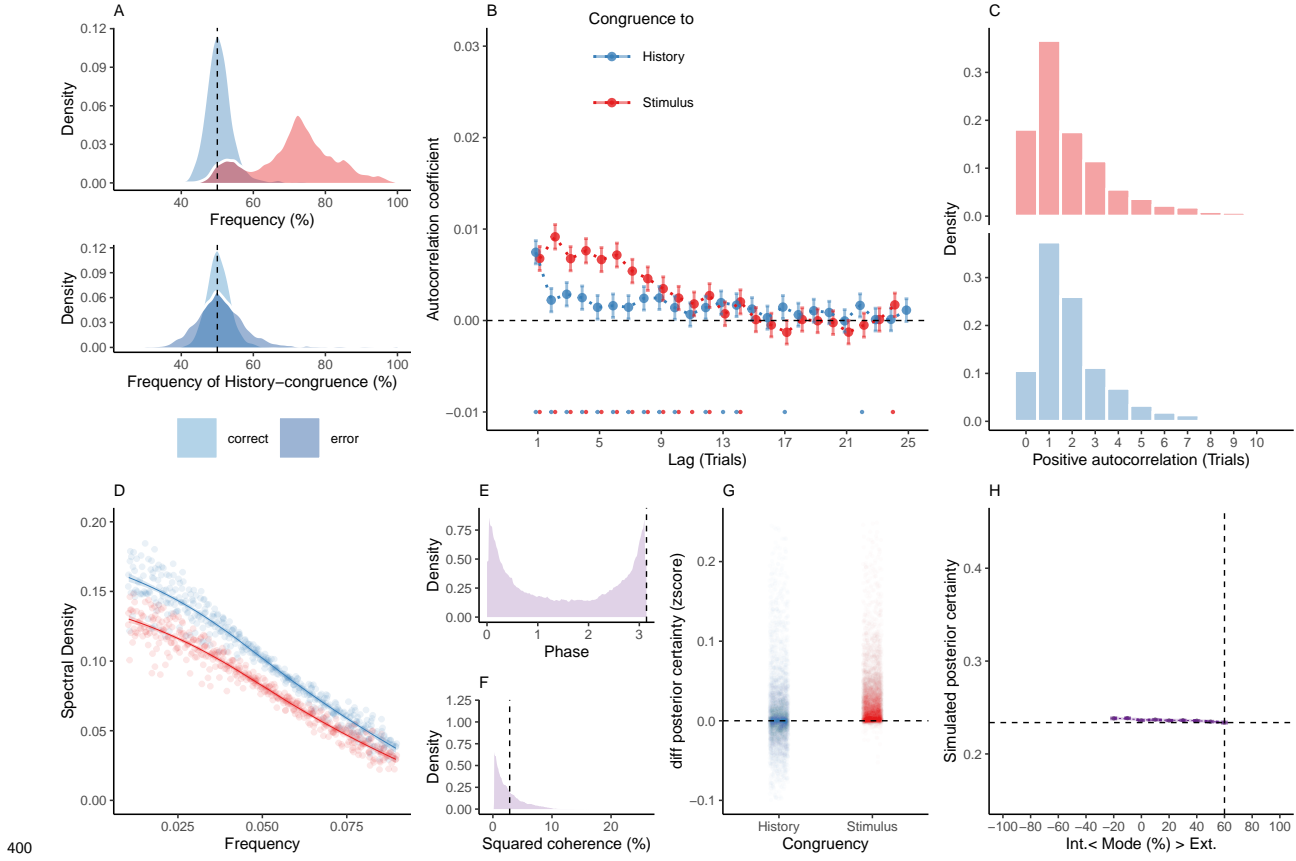
381

382 **Supplemental Figure S9. Comparison of the bimodal inference model against**
383 **reduced control models.**

384 **A. Group-level AIC.** The bimodal inference model (M1) achieved the lowest AIC
385 across the full model space ($AIC_1 = 8.16 \times 10^4$ in humans and 4.24×10^4 in mice).
386 Model M2 ($AIC_2 = 9.76 \times 10^4$ in humans and 4.91×10^4 in mice) and Model M3
387 ($AIC_3 = 1.19 \times 10^5$ in humans and 5.95×10^4 in mice) incorporated only oscillations
388 of either likelihood or prior precision. Model M4 ($AIC_4 = 1.69 \times 10^5$ in humans
389 and 9.12×10^4 in mice) lacked any oscillations of likelihood and prior precision
390 and corresponded to the normative model proposed by Glaze et al.⁵¹. In model
391 M5 ($AIC_5 = 2.01 \times 10^5$ in humans and 1.13×10^5 in mice), we furthermore removed
392 the integration of information across trials, such that perception depended only
393 in incoming sensory information.

³⁹⁴ **B. Subject-level AIC.** Here, we show the distribution of AIC values at the subject-
³⁹⁵ level. AIC for the bimodal inference model tended to be smaller than AIC for
³⁹⁶ the comparator models (statistical comparison to the second-best model M2 in
³⁹⁷ humans: $\beta = -1.71 \pm 0.19$, $T(8.57 \times 10^3) = -8.85$, $p = 1.06 \times 10^{-18}$; mice: $T(1.57 \times 10^3)$
³⁹⁸ = **-3.08**, $p = 2.12 \times 10^{-3}$).

399 **1.14 Supplemental Figure S10**



400 **Supplemental Figure S10. Reduced Control Model M2: Only oscillation of the likelihood.** When simulating data for the *likelihood-oscillation-only model*, we removed the oscillation from the prior term by setting the amplitude a_ψ to zero. Simulated data thus depended only on the participant-wise estimates for hazard rate H , amplitude a_{LLR} , frequency f , phase p and inverse decision temperature ζ .

401 A. Similar to the full model M1 (Figure 1F and Figure 4), simulated perceptual choices
 402 were stimulus-congruent in $71.97\% \pm 0.17\%$ of trials (in red). History-congruent amounted
 403 to $50.76\% \pm 0.07\%$ of trials (in blue). As in the full model, the likelihood-oscillation-only
 404 model showed a significant bias toward perceptual history $T(4.32 \times 10^3) = 10.29$, $p =$
 405 1.54×10^{-24} ; upper panel). Similarly, history-congruent choices were more frequent at error
 411 trials ($T(4.32 \times 10^3) = 9.71$, $p = 4.6 \times 10^{-22}$; lower panel).

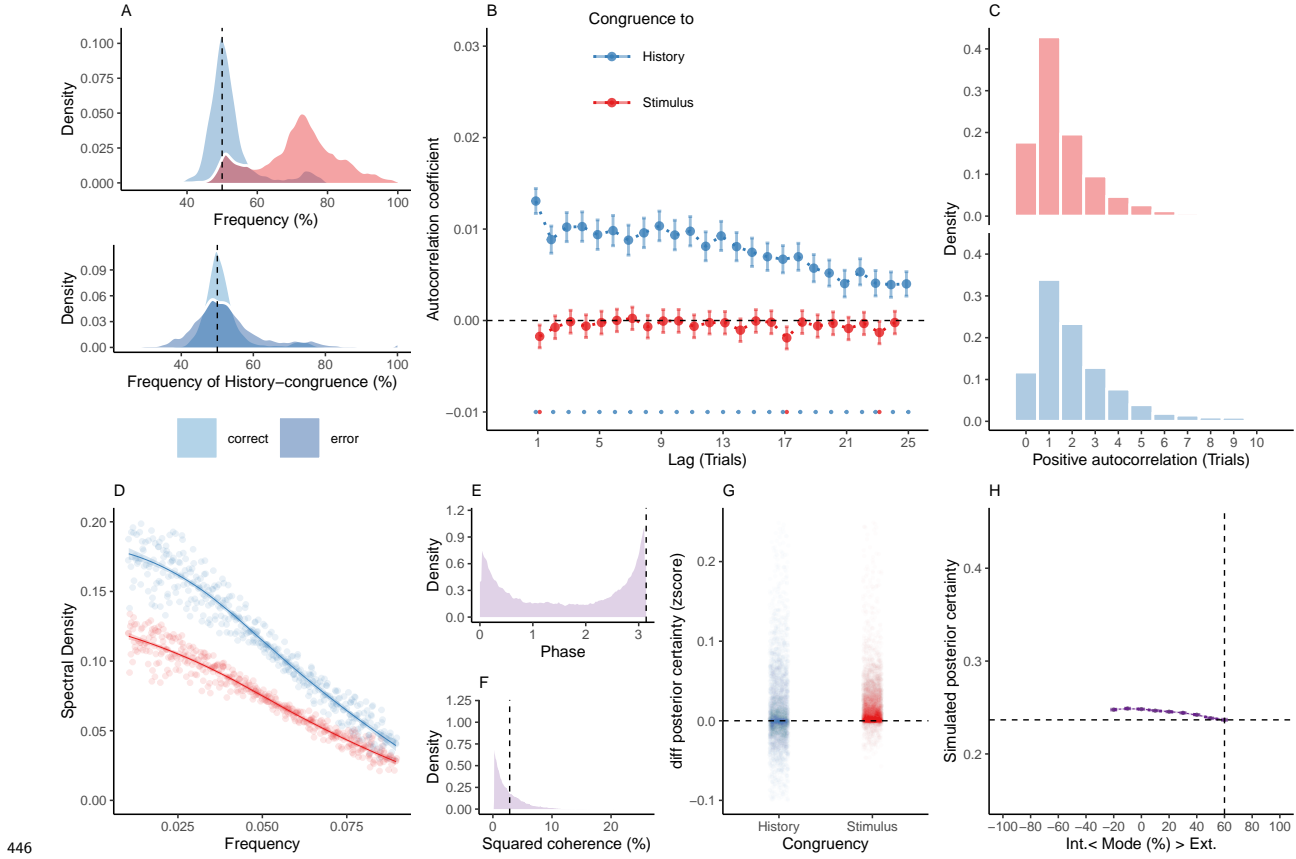
412 B. In the likelihood-oscillation-only model, we observed that the autocorrelation coefficients for

- 413 history-congruence were reduced below the autocorrelation coefficients of stimulus-congruence.
- 414 This is an approximately five-fold reduction relative to the empirical results observed in humans
- 415 (Figure 2B), where the autocorrelation of history-congruence was above the autocorrelation of
- 416 stimulus-congruence. Moreover, in the reduced model shown here, the number of consecutive
- 417 trials that showed significant autocorrelation of history-congruence was reduced to 11.
- 418 C. In the likelihood-oscillation-only model, the number of consecutive trials at which true
- 419 autocorrelation coefficients exceeded the autocorrelation coefficients for randomly permuted
- 420 data did not differ with respect to stimulus-congruence ($2.62 \pm 1.39 \times 10^{-3}$ trials; $T(4.32 \times 10^3)$
- 421 = 1.85, $p = 0.06$), but decreased with respect to history-congruence ($2.4 \pm 8.45 \times 10^{-4}$ trials;
- 422 $T(4.32 \times 10^3) = -15.26$, $p = 3.11 \times 10^{-51}$) relative to the full model.
- 423 D. In the likelihood-oscillation-only model, the smoothed probabilities of stimulus- and
- 424 history-congruence (sliding windows of ± 5 trials) fluctuated as **a scale-invariant process**
- 425 **with a 1/f power law**, i.e., at power densities that were inversely proportional to the
- 426 frequency (power $\sim 1/f^\beta$; stimulus-congruence: $\beta = -0.81 \pm 1.17 \times 10^{-3}$, $T(1.92 \times 10^5) =$
- 427 -688.65 , $p < 2.2 \times 10^{-308}$; history-congruence: $\beta = -0.79 \pm 1.14 \times 10^{-3}$, $T(1.92 \times 10^5) =$
- 428 -698.13 , $p < 2.2 \times 10^{-308}$).
- 429 E. In the likelihood-oscillation-only model, the distribution of phase shift between fluctuations
- 430 in simulated stimulus- and history-congruence peaked at half a cycle (π denoted by dotted
- 431 line). In contrast to the full model, the dynamic probabilities of simulated stimulus- and
- 432 history-congruence were positively correlated ($\beta = 2.7 \times 10^{-3} \pm 7.6 \times 10^{-4}$, $T(2.02 \times 10^6) =$
- 433 3.55 , $p = 3.8 \times 10^{-4}$).
- 434 F. In the likelihood-oscillation-only model, the average squared coherence between fluctuations
- 435 in simulated stimulus- and history-congruence (black dotted line) was reduced in comparison
- 436 to the full model ($T(3.51 \times 10^3) = -4.56$, $p = 5.27 \times 10^{-6}$) and amounted to $3.43 \pm 1.02 \times 10^{-3}\%$.
- 437 G. Similar to the full bimodal inference model, confidence simulated from the likelihood-
- 438 oscillation-only model was enhanced for stimulus-congruent choices ($\beta = 0.03 \pm 1.42 \times 10^{-4}$,

₄₃₉ $T(2.1 \times 10^6) = 191.78$, $p < 2.2 \times 10^{-308}$) and history-congruent choices ($\beta = 9.1 \times 10^{-3} \pm$
₄₄₀ 1.25×10^{-4} , $T(2.1 \times 10^6) = 72.51$, $p < 2.2 \times 10^{-308}$).

₄₄₁ H. In the likelihood-oscillation-only model, the positive quadratic relationship between the
₄₄₂ mode of perceptual processing and confidence was markedly reduced in comparison to the full
₄₄₃ model ($\beta_2 = 0.34 \pm 0.1$, $T(2.1 \times 10^6) = 3.49$, $p = 4.78 \times 10^{-4}$). The horizontal and vertical
₄₄₄ dotted lines indicate minimum posterior certainty and the associated mode, respectively.

445 **1.15 Supplemental Figure S11**



447 **Supplemental Figure S11. Reduced Control Model M3: Only oscillation of the**
 448 **prior.** When simulating data for the *prior-oscillation-only model*, we removed the oscillation
 449 from the prior term by setting the amplitude a_{LLR} to zero. Simulated data thus depended
 450 only on the participant-wise estimates for hazard rate H , amplitude a_ψ , frequency f , phase p
 451 and inverse decision temperature ζ .

452 A. Similar to the full model (Figure 1F and Figure 4), simulated perceptual choices were
 453 stimulus-congruent in $71.97\% \pm 0.17\%$ of trials (in red). History-congruent amounted to
 454 $52.1\% \pm 0.11\%$ of trials (in blue). As in the full model, the prior-oscillation-only showed a
 455 significant bias toward perceptual history $T(4.32 \times 10^3) = 18.34$, $p = 1.98 \times 10^{-72}$; upper
 456 panel). Similarly, history-congruent choices were more frequent at error trials ($T(4.31 \times 10^3)$
 457 $= 12.35$, $p = 1.88 \times 10^{-34}$; lower panel).

458 B. In the prior-oscillation-only model, we did not observe any significant positive autocor-

⁴⁵⁹ relation of stimulus-congruence , whereas the autocorrelation of history-congruence was
⁴⁶⁰ preserved.

⁴⁶¹ C. In the prior-oscillation-only model, the number of consecutive trials at which true au-
⁴⁶² tocorrelation coefficients exceeded the autocorrelation coefficients for randomly permuted
⁴⁶³ data did was decreased with respect to stimulus-congruence relative to the full model ($1.8 \pm$
⁴⁶⁴ 1.01×10^{-3} trials; $T(4.31 \times 10^3) = -6.48$, $p = 1.03 \times 10^{-10}$), but did not differ from the full
⁴⁶⁵ model with respect to history-congruence ($4.25 \pm 1.84 \times 10^{-3}$ trials; $T(4.32 \times 10^3) = 0.07$, p
⁴⁶⁶ = 0.95).

⁴⁶⁷ D. In the prior-oscillation-only model, the smoothed probabilities of stimulus- and history-
⁴⁶⁸ congruence (sliding windows of ± 5 trials) fluctuated as **a scale-invariant process with a**
⁴⁶⁹ **1/f power law**, i.e., at power densities that were inversely proportional to the frequency
⁴⁷⁰ (power $\sim 1/f^\beta$; stimulus-congruence: $\beta = -0.78 \pm 1.11 \times 10^{-3}$, $T(1.92 \times 10^5) = -706.62$, p
⁴⁷¹ $< 2.2 \times 10^{-308}$; history-congruence: $\beta = -0.83 \pm 1.27 \times 10^{-3}$, $T(1.92 \times 10^5) = -651.6$, $p <$
⁴⁷² 2.2×10^{-308}).

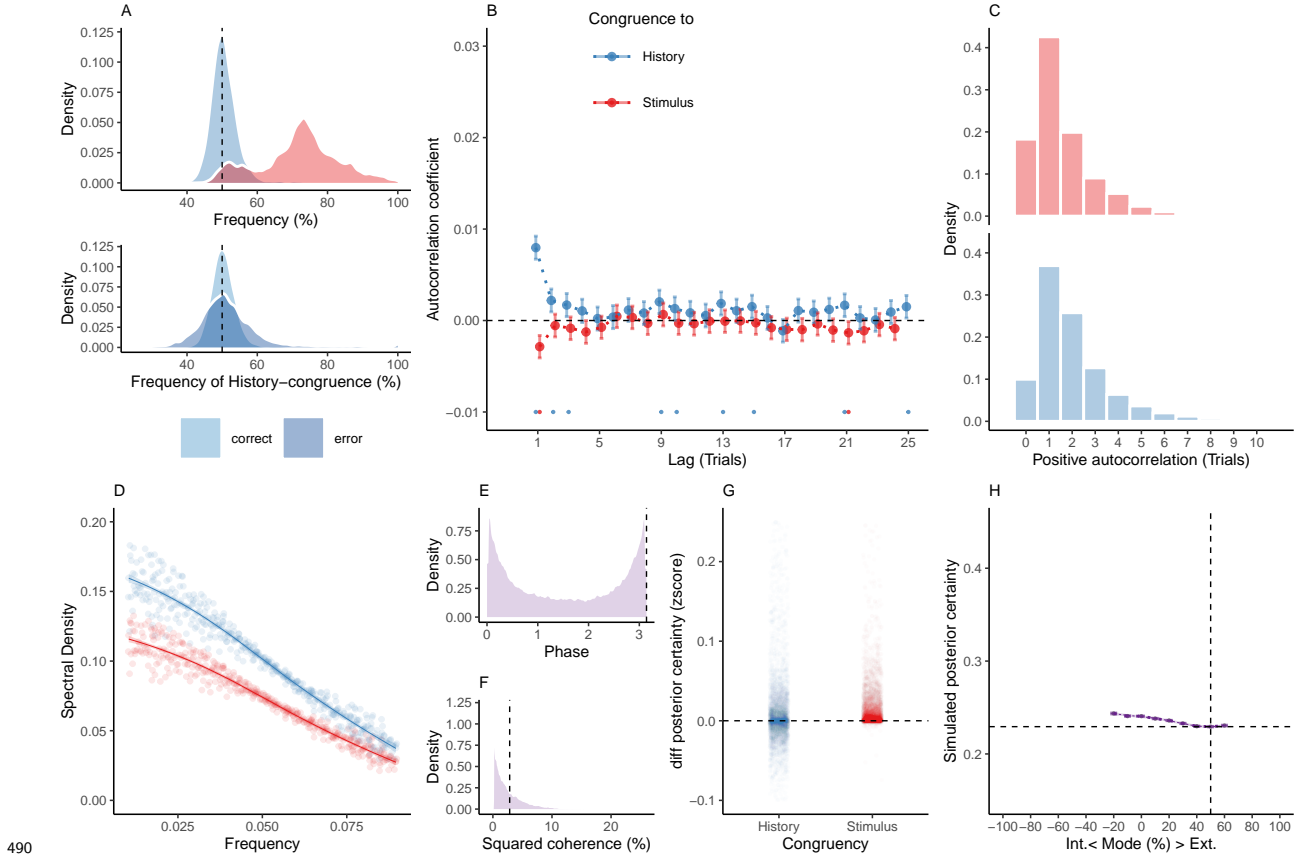
⁴⁷³ E. In the prior-oscillation-only model, the distribution of phase shift between fluctuations
⁴⁷⁴ in simulated stimulus- and history-congruence peaked at half a cycle (π denoted by dotted
⁴⁷⁵ line). Similar to the full model, the dynamic probabilities of simulated stimulus- and history-
⁴⁷⁶ congruence were anti-correlated ($\beta = -0.03 \pm 8.61 \times 10^{-4}$, $T(2.12 \times 10^6) = -34.03$, $p =$
⁴⁷⁷ 8.17×10^{-254}).

⁴⁷⁸ F. In the prior-oscillation-only model, the average squared coherence between fluctuations in
⁴⁷⁹ simulated stimulus- and history-congruence (black dotted line) was reduced in comparison to
⁴⁸⁰ the full model ($T(3.54 \times 10^3) = -3.22$, $p = 1.28 \times 10^{-3}$) and amounted to $3.52 \pm 1.04 \times 10^{-3}\%$.

⁴⁸¹ G. Similar to the full bimodal inference model, confidence simulated from the prior-oscillation-
⁴⁸² only model was enhanced for stimulus-congruent choices ($\beta = 0.02 \pm 1.44 \times 10^{-4}$, $T(2.03 \times 10^6)$
⁴⁸³ = 128.53, $p < 2.2 \times 10^{-308}$) and history-congruent choices ($\beta = 0.01 \pm 1.26 \times 10^{-4}$, $T(2.03 \times 10^6)$
⁴⁸⁴ = 88.24, $p < 2.2 \times 10^{-308}$).

⁴⁸⁵ H. In contrast to the full bimodal inference model, the prior-oscillation-only model did
⁴⁸⁶ not yield a positive quadratic relationship between the mode of perceptual processing and
⁴⁸⁷ confidence ($\beta_2 = -0.17 \pm 0.1$, $T(2.04 \times 10^6) = -1.66$, $p = 0.1$). The horizontal and vertical
⁴⁸⁸ dotted lines indicate minimum posterior certainty and the associated mode, respectively.

489 **1.16 Supplemental Figure S12**



490 **491 Supplemental Figure S12. Reduced Control Model M4: Normative evidence**

492 **accumulation.** When simulating data for the *normative-evidence-accumulation model*, we
 493 removed the oscillation from the likelihood and prior terms by setting the amplitudes a_{LLR}
 494 and a_ψ to zero. Simulated data thus depended only on the participant-wise estimates for
 495 hazard rate H and inverse decision temperature ζ .

496 A. Similar to the full model (Figure 1F and Figure 4), simulated perceptual choices were
 497 stimulus-congruent in $71.97\% \pm 0.17\%$ of trials (in red). History-congruent amounted to
 498 $50.73\% \pm 0.07\%$ of trials (in blue). As in the full model, the no-oscillation model showed
 499 a significant bias toward perceptual history $T(4.32 \times 10^3) = 9.94$, $p = 4.88 \times 10^{-23}$; upper
 500 panel). Similarly, history-congruent choices were more frequent at error trials ($T(4.31 \times 10^3)$
 501 $= 10.59$, $p = 7.02 \times 10^{-26}$; lower panel).

502 B. In the normative-evidence-accumulation model, we did not find significant autocor-

503 relations for stimulus-congruence. Likewise, we did not observe any autocorrelation of
504 history-congruence beyond the first three consecutive trials.

505 C. In the normative-evidence-accumulation model, the number of consecutive trials at
506 which true autocorrelation coefficients exceeded the autocorrelation coefficients for randomly
507 permuted data decreased with respect to both stimulus-congruence ($1.8 \pm 1.59 \times 10^{-3}$ trials;
508 $T(4.31 \times 10^3) = -5.21$, $p = 2 \times 10^{-7}$) and history-congruence ($2.18 \pm 5.48 \times 10^{-4}$ trials;
509 $T(4.32 \times 10^3) = -17.1$, $p = 1.75 \times 10^{-63}$) relative to the full model.

510 D. In the normative-evidence-accumulation model, the smoothed probabilities of stimulus- and
511 history-congruence (sliding windows of ± 5 trials) fluctuated as **a scale-invariant process**
512 **with a $1/f$ power law**, i.e., at power densities that were inversely proportional to the
513 frequency (power $\sim 1/f^\beta$; stimulus-congruence: $\beta = -0.78 \pm 1.1 \times 10^{-3}$, $T(1.92 \times 10^5) =$
514 -706.93 , $p < 2.2 \times 10^{-308}$; history-congruence: $\beta = -0.79 \pm 1.12 \times 10^{-3}$, $T(1.92 \times 10^5) =$
515 -702.46 , $p < 2.2 \times 10^{-308}$).

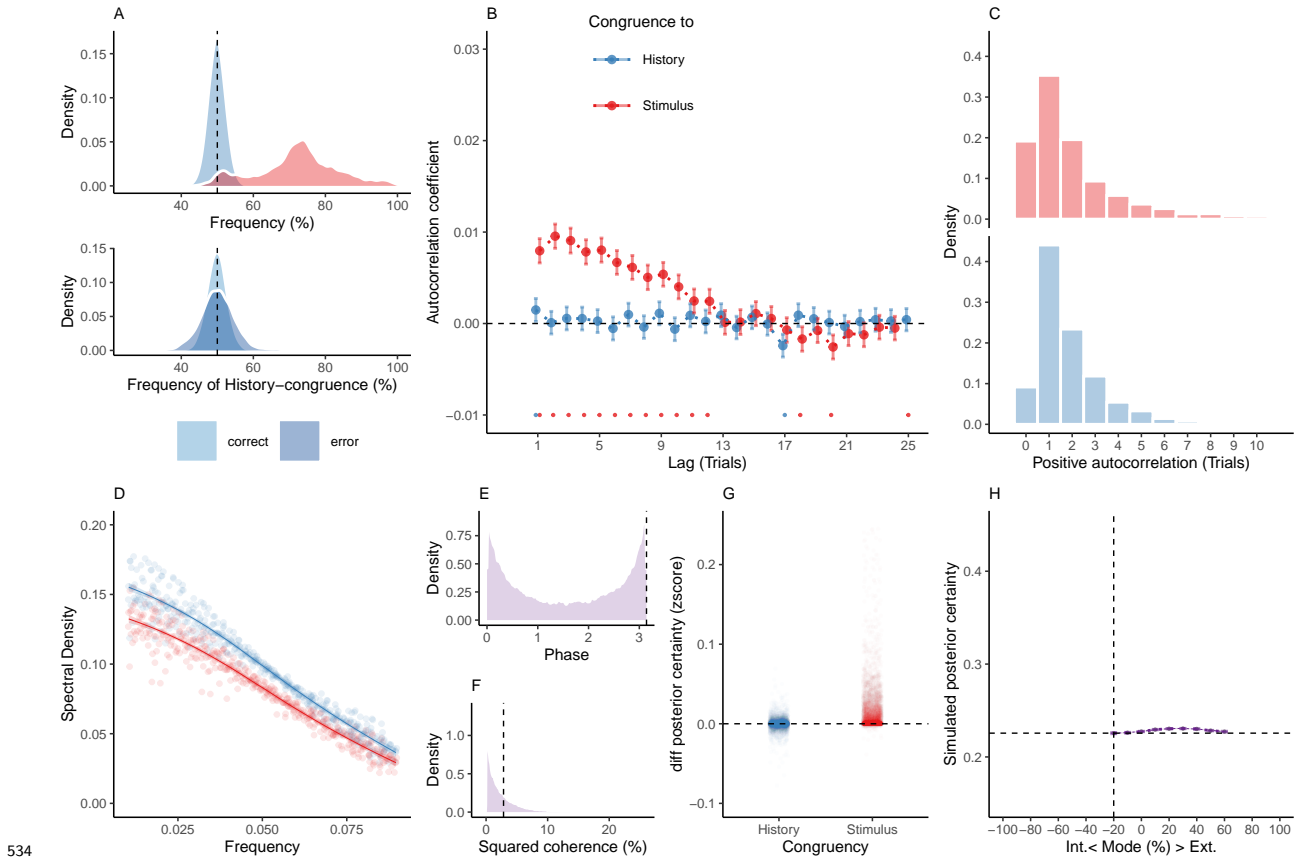
516 E. In the normative-evidence-accumulation model, the distribution of phase shift between
517 fluctuations in simulated stimulus- and history-congruence peaked at half a cycle (π denoted
518 by dotted line). In contrast to the full model, the dynamic probabilities of simulated stimulus-
519 and history-congruence were positively correlated ($\beta = 4.3 \times 10^{-3} \pm 7.97 \times 10^{-4}$, $T(1.98 \times 10^6)$
520 $= 5.4$, $p = 6.59 \times 10^{-8}$).

521 F. In the normative-evidence-accumulation model, the average squared coherence between
522 fluctuations in simulated stimulus- and history-congruence (black dotted line) was reduced in
523 comparison to the full model ($T(3.52 \times 10^3) = -6.27$, $p = 3.97 \times 10^{-10}$) and amounted to
524 $3.26 \pm 8.88 \times 10^{-4}\%$.

525 G. Similar to the full bimodal inference model, confidence simulated from the no-oscillation
526 model was enhanced for stimulus-congruent choices ($\beta = 0.01 \pm 1.05 \times 10^{-4}$, $T(2.1 \times 10^6)$
527 $= 139.17$, $p < 2.2 \times 10^{-308}$) and history-congruent choices ($\beta = 8.05 \times 10^{-3} \pm 9.2 \times 10^{-5}$,
528 $T(2.1 \times 10^6) = 87.54$, $p < 2.2 \times 10^{-308}$).

⁵²⁹ H. In the normative-evidence-accumulation model, the positive quadratic relationship between
⁵³⁰ the mode of perceptual processing and confidence was markedly reduced in comparison to
⁵³¹ the full model ($\beta_2 = 0.14 \pm 0.07$, $T(2.1 \times 10^6) = 1.95$, $p = 0.05$). The horizontal and vertical
⁵³² dotted lines indicate minimum posterior certainty and the associated mode, respectively.

533 **1.17 Supplemental Figure S13**



534 **535 Supplemental Figure S13. Reduced Control Model M5: No accumulation of
536 information across trials.** When simulating data for the *no-evidence-accumulation model*,
537 we removed the accumulation of information across trials by setting the Hazard rate H to
538 0.5. Simulated data thus depended only on the participant-wise estimates for the amplitudes
539 $a_{LLR/\psi}$, frequency f , phase p and inverse decision temperature ζ .

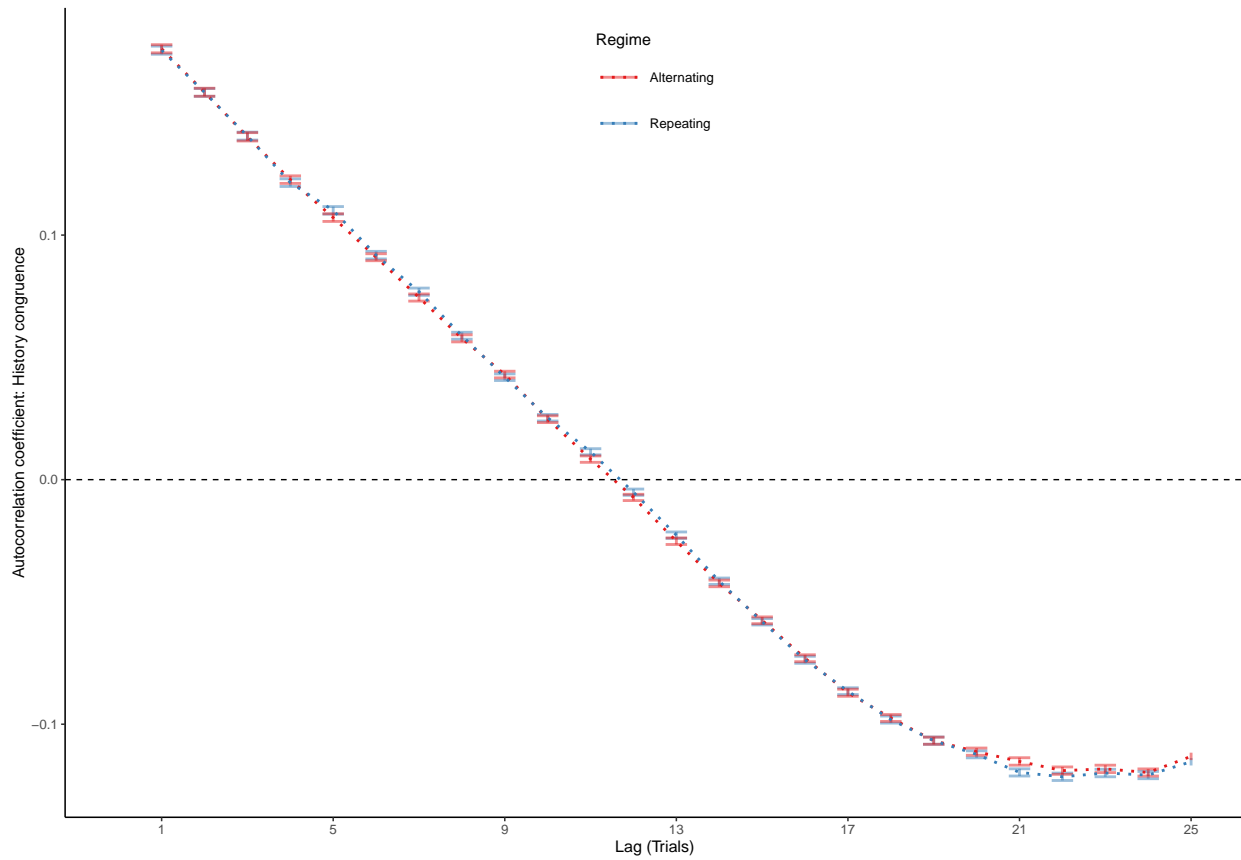
540 A. Similar to the full model (Figure 1F and Figure 4), simulated perceptual choices were
541 stimulus-congruent in $72.14\% \pm 0.17\%$ of trials (in red). History-congruent amounted to
542 $49.89\% \pm 0.03\%$ of trials (in blue). In contrast to the full model, the no-accumulation model
543 showed a significant bias against perceptual history $T(4.32 \times 10^3) = -3.28$, $p = 1.06 \times 10^{-3}$;
544 upper panel). In contrast to the full model, there was no difference in the frequency of
545 history-congruent choices between correct and error trials ($T(4.31 \times 10^3) = 0.76$, $p = 0.44$;
546 lower panel).

- 547 B. In the no-evidence-accumulation model, we found no significant autocorrelation of history-
 548 congruence beyond the first trial, whereas the autocorrelation of stimulus-congruence was
 549 preserved.
- 550 C. In the no-evidence-accumulation model, the number of consecutive trials at which true
 551 autocorrelation coefficients exceeded the autocorrelation coefficients for randomly permuted
 552 data increased with respect to stimulus-congruence ($2.83 \pm 1.49 \times 10^{-3}$ trials; $T(4.31 \times 10^3) =$
 553 3.45 , $p = 5.73 \times 10^{-4}$) and decreased with respect to history-congruence ($1.85 \pm 3.49 \times 10^{-4}$
 554 trials; $T(4.32 \times 10^3) = -19.37$, $p = 3.49 \times 10^{-80}$) relative to the full model.
- 555 D. In the no-evidence-accumulation model, the smoothed probabilities of stimulus- and
 556 history-congruence (sliding windows of ± 5 trials) fluctuated as **a scale-invariant process**
 557 **with a 1/f power law**, i.e., at power densities that were inversely proportional to the
 558 frequency (power $\sim 1/f^\beta$; stimulus-congruence: $\beta = -0.82 \pm 1.2 \times 10^{-3}$, $T(1.92 \times 10^5) =$
 559 -681.98 , $p < 2.2 \times 10^{-308}$; history-congruence: $\beta = -0.78 \pm 1.11 \times 10^{-3}$, $T(1.92 \times 10^5) =$
 560 -706.57 , $p < 2.2 \times 10^{-308}$).
- 561 E. In the no-evidence-accumulation model, the distribution of phase shift between fluctuations
 562 in simulated stimulus- and history-congruence peaked at half a cycle (π denoted by dotted
 563 line). In contrast to the full model, the dynamic probabilities of simulated stimulus- and
 564 history-congruence were not significantly anti-correlated ($\beta = 6.39 \times 10^{-4} \pm 7.22 \times 10^{-4}$,
 565 $T(8.89 \times 10^5) = 0.89$, $p = 0.38$).
- 566 F. In the no-evidence-accumulation model, the average squared coherence between fluctuations
 567 in simulated stimulus- and history-congruence (black dotted line) was reduced in comparison
 568 to the full model ($T(3.56 \times 10^3) = -9.96$, $p = 4.63 \times 10^{-23}$) and amounted to $2.8 \pm 7.29 \times 10^{-4}\%$.
- 569 G. Similar to the full bimodal inference model, confidence simulated from the no-evidence-
 570 accumulation model was enhanced for stimulus-congruent choices ($\beta = 0.01 \pm 9.4 \times 10^{-5}$,
 571 $T(2.11 \times 10^6) = 158.1$, $p < 2.2 \times 10^{-308}$). In contrast to the full bimodal inference model,
 572 history-congruent choices were not characterized by enhanced confidence ($\beta = 8.78 \times 10^{-5} \pm$

₅₇₃ 8.21×10^{-5} , $T(2.11 \times 10^6) = 1.07$, $p = 0.29$).

₅₇₄ H. In the no-evidence-accumulation model, the positive quadratic relationship between the
₅₇₅ mode of perceptual processing and confidence was markedly reduced in comparison to the full
₅₇₆ model ($\beta_2 = 0.19 \pm 0.06$, $T(2.11 \times 10^6) = 3$, $p = 2.69 \times 10^{-3}$). The horizontal and vertical
₅₇₇ dotted lines indicate minimum posterior certainty and the associated mode, respectively.

578 **1.18 Supplemental Figure S14**



579
580 **Supplemental Figure S14. Autocorrelation of history-congruence of alternating**
581 **and repeating biases.** Here, we simulate the autocorrelation of history-congruence in 10^3
582 synthetic participants. In the repeating regime (blue), history-congruence fluctuated between
583 50% and 80% (blue) in interleaved blocks (10 blocks per condition with a random duration
584 between 15 and 30 trials). In the alternation regime (red), history-congruence fluctuated
585 between 50% and 20%. The resulting autocorrelation curves for history-congruence overlap,
586 indicating that our analysis is able to accommodate both repeating and alternating biases.

⁵⁸⁷ 1.19 Supplemental Table T1

| Authors | Journal | Year |
|--|--|------|
| Bang, Shekhar, Rahnev | JEP:General | 2019 |
| Bang, Shekhar, Rahnev | JEP:General | 2019 |
| Calder-Travis, Charles, Bogacz, Yeung | Unpublished | NA |
| Clark & Merfeld | Journal of Neurophysiology | 2018 |
| Clark | Unpublished | NA |
| Faivre, Filevich, Solovey, Kuhn, Blanke | Journal of Neuroscience | 2018 |
| Faivre, Vuillaume, Blanke, Cleeremans | bioRxiv | 2018 |
| Filevich & Fandakova | Unplublished | NA |
| Gajdos, Fleming, Saez Garcia, Weindel, Davranche | Neuroscience of Consciousness | 2019 |
| Gherman & Philiastides | eLife | 2018 |
| Haddara & Rahnev | PsyArXiv | 2020 |
| Haddara & Rahnev | PsyArXiv | 2020 |
| Hainguerlot, Vergnaud, & de Gardelle | Scientific Reports | 2018 |
| Hainguerlot, Gajdos, Vergnaud, & de Gardelle | Unpublished | NA |
| Jachs, Blanco, Grantham-Hill, Soto | JEP:HPP | 2015 |
| Jachs, Blanco, Grantham-Hill, Soto | JEP:HPP | 2015 |
| Jachs, Blanco, Grantham-Hill, Soto | JEP:HPP | 2015 |
| Jaquiere, Yeung | Unpublished | NA |
| Kvam, Pleskac, Yu, Busemeyer | PNAS | 2015 |
| Kvam, Pleskac, Yu, Busemeyer | PNAS | 2015 |
| Kvam and Pleskac | Cognition | 2016 |
| Law, Lee | Unpublished | NA |
| Lebreton, et al. | Sci. Advances | 2018 |
| Lempert, Chen, & Fleming | PlosOne | 2015 |
| Locke*, Gaffin-Cahn*, Hosseiniaveh, Mamassian, & Landy | Attention, Perception, & Psychophysics | 2020 |
| Maniscalco, McCurdy,Odegaard, & Lau | J Neurosci | 2017 |
| Maniscalco, McCurdy,Odegaard, & Lau | J Neurosci | 2017 |
| Maniscalco, McCurdy,Odegaard, & Lau | J Neurosci | 2017 |
| Maniscalco, McCurdy,Odegaard, & Lau | J Neurosci | 2017 |
| Martin, Hsu | Unpublished | NA |
| Massoni & Roux | Journal of Mathematical Psychology | 2017 |
| Massoni | Unpublished | NA |
| Mazor, Friston & Fleming | eLife | 2020 |
| Mei, Rankine,Olafsson, Soto | bioRxiv | 2019 |
| Mei, Rankine,Olafsson, Soto | bioRxiv | 2019 |
| O'Hora, Zgonnikov, Kenny, Wong-Lin | Fechner Day proceedings | 2017 |
| O'Hora, Zgonnikov, CiChocki | Unpublished | NA |

(continued)

| Authors | Journal | Year |
|--|--|------|
| O'Hora, Zgonnikov, Neverauskaite | Unpublished | NA |
| Palser et al | Consciousness & Cognition | 2018 |
| Pereira, Faivre, Iturrate et al. | bioRxiv | 2018 |
| Prieto et al. | Submitted | NA |
| Rahnev et al | J Neurophysiol | 2013 |
| Rausch & Zehetleitner | Front Psychol | 2016 |
| Rausch et al | Attention, Perception, & Psychophysics | 2018 |
| Rausch et al | Attention, Perception, & Psychophysics | 2018 |
| Rausch, Zehetleitner, Steinhauser, & Maier | NeuroImage | 2020 |
| Recht, de Gardelle & Mamassian | Unpublished | NA |
| Reyes et al. | PlosOne | 2015 |
| Reyes et al. | Submitted | NA |
| Rouault, Seow, Gillan, Fleming | Biol. Psychiatry | 2018 |
| Rouault, Seow, Gillan, Fleming | Biol. Psychiatry | 2018 |
| Rouault, Dayan, Fleming | Nat Commun | 2019 |
| Sadeghi et al | Scientific Reports | 2017 |
| Schmidt et al. | Consc Cog | 2019 |
| Shekhar & Rahnev | J Neuroscience | 2018 |
| Shekhar & Rahnev | PsyArXiv | 2020 |
| Sherman et al | Journal of Neuroscience | 2016 |
| Sherman et al | Journal of Cognitive Neuroscience | 2016 |
| Sherman et al | Unpublished | NA |
| Sherman et al | Unpublished | NA |
| Siedlecka, Wereszczyski, Paulewicz, Wierzchon | bioRxiv | 2019 |
| Song et al | Consciousness & Cognition | 2011 |
| van Boxtel, Orchard, Tsuchiya | bioRxiv | 2019 |
| van Boxtel, Orchard, Tsuchiya | bioRxiv | 2019 |
| Wierzchon, Paulewicz, Asanowicz, Timmermans & Cleeremans | Consciousness and Cognition | 2014 |
| Wierzchon, Anzulewicz, Hobot, Paulewicz & Sackur | Consciousness and Cognition | 2019 |

⁵⁸⁸ 1.20 Supplemental Table T2

| Parameters | Interpretation |
|------------|---|
| α | Sensitivity to sensory information |
| H | Expected probability of a switch in the cause of sensory information (Hazard) |
| a_{LLR} | Amplitude of fluctuations in likelihood precision ω_{LLR} |
| a_ψ | Amplitude of fluctuations in prior precision ω_ψ |
| f | Frequency of ω_{LLR} and ω_ψ |
| p | Phase (p for ω_{LLR} ; p + π for ω_ψ) |
| ζ | Inverse decision temperature |